

Exergy analysis of a gas-turbine combined-cycle power plant with precombustion CO₂ capture

Ivar S. Ertesvåg,^{a,*} Hanne M. Kvamsdal,^b Olav Bolland^a

^a Department of Energy and Process Engineering,
Norwegian University of Science and Technology,
NO-7491 Trondheim, Norway

^b SINTEF Energy Research,
NO-7465 Trondheim, Norway

(Received 21 November 2003, final version 21 May 2004) - Accepted for publication in Energy

Abstract A concept for natural-gas (NG) fired power plants with CO₂ capture was investigated using exergy analysis. NG was reformed in an autothermal reformer (ATR), and the CO₂ was separated before the hydrogen-rich fuel was used in a conventional combined-cycle (CC) process. The main issue of the study was to investigate the integration of the reforming process and the combined cycle. A corresponding conventional CC power plant with no CO₂ capture was simulated for comparison. A Base Case with CO₂ capture was specified with turbine-inlet temperature (TIT) of 1250 °C and an air-compressor outlet pressure of 15.6 bar. In this case, the net electric-power production was 48.9% of the lower heating value (LHV) of the NG or 46.9% of its chemical exergy. The captured and compressed CO₂ (200 bar) represented 3.1% of the NG chemical exergy, while the NG, due to its pressure (50 bar) had a physical exergy equal to 1.0% of its chemical exergy. The effects of changed NG composition and environmental temperature were investigated. Higher pressure in the gas-turbine and reformer increased the combustion in the ATR and reduced the overall efficiency. Supplementary firing (SF) was investigated as an alternative means of heating the ATR. This also reduced the efficiency. Heating the feeds of the ATR with its product stream was shown to reduce the irreversibility and improve the efficiency of the plant. Both this, and the effect of increased TIT to 1450 °C were investigated. Combining both measures, the net electric-power production was increased to 53.3% of the NG LHV or 51.1% of the NG chemical exergy. On the other hand, both increased TIT and the ATR product-feed heat exchange reduced the conversion of hydrocarbons to CO₂.

1 Introduction

Man-made emissions of CO₂ and their possible environmental effects cause great concern. On the one hand, international agreements imply reduction of CO₂ emissions. On the other hand, the general use of electric power, mainly produced from fossil-fuel power plants, increases worldwide. One possible remedy is to construct fossil-fuel based power plants that do not emit the CO₂ that is produced.

In order to reduce the CO₂ emissions from natural-gas (NG) based power-generation plants, three different approaches have emerged as the most promising:

A) Separation of CO₂ from the exhaust gas of a standard gas-turbine combined cycle (CC), using chemical absorption by amine solutions. This approach has been widely treated in the literature (see [1-3]) and can be applied to existing, conventional plants.

B) Oxy-fuel CC with a close-to-stoichiometric combustion with high-purity oxygen from an air-separation plant [3,4]. As the combustion products are CO₂ and water vapor, in principle, CO₂ can be captured simply by

* Author for correspondence, fax: +4773593580, e-mail: ivar.s.ertesvag@ntnu.no

condensing water from the flue gas. In this approach, CO₂ is used as the main working fluid of the CC. This presents considerable challenges, especially in combustion technology.

C) Precombustion decarbonization and CO₂ capture, where the carbon of the NG is removed prior to combustion and the fuel heating value is transferred to hydrogen by reforming [5-12]. The hydrogen-rich mixture is combusted in a conventional CC power plant.

Some of the work on CO₂-emissions reduction is related to coal-fired plants, often with integrated gasification of the fuel. This is because coal is the dominating fossil fuel in power stations. However, some of the technology is generic and may be developed for NG firing and later utilized for coal firing. There are several reasons why NG firing is studied; three of these are: Natural-gas fired combined cycles are much closer to realization as pilot plants with CO₂ capture than plants with coal gasification. Second, it has been argued [3] that the specific cost of CO₂ capture is lower in an NG-fuelled plant than in a coal-fired plant. Third, the present study was also motivated by the specific Norwegian situation, with no coal-fired plants and large resources of NG.

Other approaches (e.g., fuel cells) and variants of those mentioned above can be found in literature. For instance, precombustion decarbonization can be achieved with steam reforming, with partial oxidation, or with auto-thermal reforming, and the subsequent CO₂-separation can be achieved by chemical absorption or by physical absorption [8]. Future alternatives also include a combination of H₂-separating membranes and steam reforming [13].

A common challenge for all approaches is the reduced efficiency in terms of net electric-power production per unit of fuel energy. Moreover, the separated CO₂ has to be compressed, transported, and deposited.

The present work focuses on approach C; decarbonization prior to combustion (precombustion). The motivation behind this concept is to utilize known technology. In ammonia production, for example, hydrogen is produced by the reforming of NG and the subsequent removal of the CO₂. In the process that is described and analyzed in the following, this technology was used to produce fuel for a conventional combined-cycle power plant, and the two processes are integrated. Some preliminary investigations have been presented in [10-12].

A similar power plant has also been investigated by Lozza and Chiesa [8,9] with reforming by partial oxidation and by steam reforming. In the present study, a process with auto-thermal reforming is investigated. Auto-thermal reforming uses some steam for reforming, although less than in steam reforming. Heat and some water vapor are supplied by burning of some of the fuel, however, less fuel is oxidated than with the partial oxidation method. The study is an investigation of the integration between the reformer section and the gas-turbine (GT) and steam-turbine (ST) power cycles.

A detailed second-law analysis or exergy analysis has been performed in addition to a first-law analysis in order to analyze this complex energy system more thoroughly. The exergy analysis quantifies and localizes the thermodynamic losses (irreversibilities). Such knowledge is useful in explaining the changes observed in a parameter variation and in explaining the differences between the various processes. This is particularly useful when dealing with new processes where little or no experience has been gained. When the detailed breakdown of thermodynamic losses has been found, appropriate measures can be taken to improve the plant. Moreover, an exergy analysis reveals the thermodynamic value of a separated substance (e.g. captured CO₂) and also the value of a pressurized gas (e.g. the supplied NG), which both are not notified in a 1st-law analysis.

2 Process description

The flowsheet of the combined-cycle (CC) process with hydrocarbon reforming is shown in Fig. 1. Natural gas (NG) is reformed to a mixture of CO₂, H₂, H₂O, and N₂. The major part of the H₂O and CO₂ is removed, and the hydrogen-rich fuel is combusted in a gas turbine (GT). The exhaust is ducted through a steam generator

with a possibility for supplementary firing. The steam generator is integrated with the reforming process, and the steam is utilized in a three-pressure-level power cycle.

First, the NG is expanded in an expander from the supply pressure to the pressure of the reforming section, which is determined by the pressure ratio of the GT. Alternatively, this pressure reduction may be achieved by throttling. After expansion, the fuel is heated using low-temperature heat from cooling water coming from the condenser or the CO₂ compressors. The NG expansion and reheat (prior to stream 1) is not shown in the flowsheet. In the reforming section, NG (stream 1) is merged in the mixer (MIX) with steam (35) at the same pressure and preheated by the exhaust-gas stream in the pre-heater before entering the pre-reformer (PRE). Air (8) extracted from the gas-turbine air-compressor (AC) and the PRE products (4) are also preheated by the exhaust-gas before entering the auto-thermal reformer (ATR). In the present study, the preheater in front of the heat-recovery steam generator (HRSG) was modeled as a four-fluid heat exchanger. Heat is transferred from the turbine-exhaust gas to the PRE feed and the two ATR feeds (*i.e.* PRE products and extracted air). In the pre-reformer, most of the heavier hydrocarbon components (mainly ethane and propane) are converted to H₂, CO, and CO₂, whereas the remaining methane is to be converted in the ATR unit. The steam cycle takes advantage of the reforming process by utilizing the cooling process of the reformer products downstream of the ATR to generate additional saturated high-pressure (HP) steam in the heat exchangers H1, H2, and H4 (streams 36–41). Water is pumped from low pressure (LP) to HP (stream 36), heated and evaporated, and the saturated steam (42) is fed into the HP steam drum. Below, a variant configuration (not shown in the flowsheet) will also be investigated, where the ATR outlet (11), before entering H1, will be used for preheating the ATR feed (5 and 10).

The CO produced in the reforming process is converted to CO₂ in the high- and low-temperature shift reactors (HTS, LTS). Most of the water is removed (stream 43) in the water-removal unit (WR) by condensation at a low temperature. A large fraction of the CO₂ content is removed (44) in the chemical absorber unit (ABS). The captured CO₂ is compressed in three steps with intercooling, then cooled to liquid state, and finally pumped to the transportation pressure. The compression of CO₂ (from stream 44) is not shown in the flowsheet in Fig. 1.

The required gas-turbine fuel-nozzle pressure is typically 25% higher than the pressure of the air from the gas-turbine compressor outlet. Thus, an extra pressurization of the fuel is required, and a fuel compressor (FC) is placed downstream the reforming and absorption sections. The fuel is heated by the LTS feed stream (14) and then fed (23) into the GT combustor. The steam cycle, comprising the heat-recovery steam generator (HRSG), the steam turbines (ST), and the seawater-cooled condenser (COND), has three pressure levels and steam reheat. In the present simulations, the HRSG was modeled as a sequence of a three-fluid heat exchanger for HP and medium-pressure (MP) superheating, an HP boiler, a four-fluid heat exchanger for combined HP water heating and MP superheating, and five heat exchangers for, respectively, LP superheating, MP boiling, MP water heating, LP boiling, LP water heating, and low-temperature (make-up and LP) water heating. These details, including the arrangement of pumps, are not shown in the flowsheet.

The reforming process is supplied with pressurized air (stream 8) and steam (35). The power cycles and the reforming process are further integrated with respect to preheating of feed streams for the reformers (ATR and PRE). The heat required in the reforming process is partly supplied by preheating of the reformer feed streams, and partly by the exothermic reaction (combustion) between oxygen and NG in the ATR. The combustion may also take place in front of the preheating section of the HRSG by supplementary firing (SF). For a conventional CC plant, it is known that SF reduces the efficiency. However, this is not so obvious for the process given in Fig. 1. The alternative to SF is increased extraction of air from the gas-turbine compressor to the combustion of NG in the ATR, which also decreases the efficiency of the CC. The present study evaluates methods of supplying heat for the reforming process.

The steam used in reforming (stream 35) has to be compensated by make-up water (34). In effect, this relatively large amount of cold freshwater is evaporated and superheated in the steam cycle to be used in the reforming process. Some of the make-up water can be supplied from the condensate drained from the reformed fuel (43).

The resulting fuel mixture (stream 20) contains mainly H₂ and N₂. It also contains minor amounts of CO, CO₂, and methane, and trace amounts of other hydrocarbons. Compared with conventional NG firing of gas turbines, the air volumetric flow is reduced by the air extraction for the reforming section (stream 8). However, this is compensated by the increased fuel volumetric flow. It is, therefore, possible to maintain the GT pressure ratio at approximately the same level as for a conventional NG fired gas turbine with no air extraction.

It can be noted that the temperature difference in heat exchanger H1 is quite high, as will be seen below. The ATR outlet at a high temperature exchanges heat with boiling water at HP, that is, at a much lower temperature. This arrangement, which is common in engineering practice, depends on the material properties. Generally, heat exchange at high temperatures is challenging for the material. A liquid at one side will keep the temperature of the material close to that of the liquid. The main reason for selecting the arrangement in the present case is metal dusting. This is a corrosion phenomenon which leads to the disintegration of alloys. It occurs particularly when metals at a high temperature are exposed to a gas containing hydrogen. Thus, the heat is exchanged with a liquid to avoid a high temperature in the heat exchanger material. The possibility of another arrangement, with a presumption of advanced materials or coating, will also be investigated.

The process shown in Fig. 1 can readily be simplified to a conventional natural-gas fired combined cycle. Then, NG fuel is expanded from the supply pressure and fed directly into the combustor (23). That is, no steam (35) or air (8) is added, no reforming and no separation take place, and no heat exchange with the fuel takes place except for the possibility of preheating. This conventional process was simulated for comparison.

3 Methodology

The process shown in Fig.1 was modeled in PRO/II v.5.6 (SIMSCI Inc.). The flowsheet simulations provided data for species mass flows and energy flows. The CO₂ compression was simulated in a separate model set up with the same program.

The gas-turbine (GT) model in the combined cycle (CC) was based on the GTPRO (Thermoflow Inc.) gas-turbine database for the General Electric (GE) 9351FA technology. This gas turbine represents modern technology today, and it is used in a number of plants built in the last few years.

The pre-reformer (PRE), the main reformer (ATR), and the shift reactors (HTS, LTS) were assumed to be equilibrium reactors. The GT combustor and the supplementary firing were also calculated as equilibrium reactors. However, with high oxygen excess, the result can be regarded as complete combustion.

Pressure drops of 3% were assumed in each of the pre-reformer, shift-reactors, and heat exchangers, whereas a 6% pressure drop was assumed in the ATR. For the GT combustor, the air inlet pressure was set to 1% above the outlet pressure, while the fuel inlet pressure was approximately 25% above the outlet pressure.

The pressure-volume-temperature relation of the substances was modeled by a Soave-Redlich-Kwong equation of state. For mixtures, this was combined with Kay's rule. These thermodynamic models were provided with PRO/II. Gas flows with chemical reactions are often modeled with an ideal-gas approximation. However, at high pressure or with a large content of water vapor, there may be considerable real-gas effects.

The compression of CO₂ was accomplished using a 3-step intercooled compression and subsequent pumping. The compressor polytropic efficiencies ranged from 75% (high pressure) to 85% (low pressure). The heat exchangers were modeled with 3% pressure loss as in the rest of the study. After each intercooler, condensed water was separated from the CO₂ in flash tanks.

The generator efficiency was assumed equal to 98.6%. The auxiliary power, mainly power for cooling-water pumps, was set to 1% of the heat transferred to the coolant in the condenser and the CO₂-compression intercoolers (cf. [8]).

The generator losses, auxiliary power, power for compressing of the removed CO₂, and hence, the net electric power production, were calculated separately after the process simulation.

The flowsheet simulations also provided the necessary data for calculating the physical (thermomechanical) exergy. Based on these data, the chemical exergy was calculated in a separate, in-house program according to the theory given, see, for example [14]. The chemical exergy of the individual species in this study were taken from [14] and corrected to the ambient temperature of 8 °C according to the procedure given by Kotas [14,15]. The composition of the dry atmosphere was defined by the molar fractions (%) N₂: 78.03, O₂: 20.99, Ar: 0.94, CO₂: 0.03. For the present simulations, the content of water vapor corresponds to a relative humidity of 82% at 8 °C and 1 atm, which was chosen as the environmental temperature and pressure. This was the state of the air entrained into the system. The exergy values of all streams were calculated from this. The irreversibility was then found from the exergy balance for each of the individual unit processes.

It should be noted that the chemical exergy was calculated with reference to the atmosphere. Special care has to be taken when inspecting the values for substances that occur in liquid state, that is, water in the steam cycle and captured CO₂ compressed and liquefied for deposit: For consistency throughout the entire process, the chemical exergies of these substances were determined as if they were gaseous. Then the negative exergy due to condensing was included in the thermomechanical exergy. Accordingly, the total exergy might be less than the chemical exergy. Alternatively, the phase-change exergy could have been included in the chemical exergy. In either case, the total exergy will be the same.

4 Present predictions

4.1 Fuel and environment

The chosen composition of the natural gas (NG) was 83.89% methane, 5.34% CO₂, 0.01% H₂O, and 2.65% nitrogen, 4.87% ethane, 2.12% propane, 0.50% n-butane, 0.28% iso-butane, 0.11% n-pentane, 0.12% iso-pentane, 0.06% n-hexane, 0.04% n-heptane, and 0.01% n-octane. This composition is a possible NG from the Norwegian sector. Specifications for traded NG may contain less CO₂ and less higher hydrocarbons than listed here. The lower heating value (LHV) and chemical exergy of this mixture were calculated to 818901 kJ/kmol and 853085 kJ/kmol, respectively, and the molar mass was 19.674 kg/kmol.

The supply pressure and temperature of the NG was set to 50 bar and 4 °C. The thermomechanical exergy at this state was calculated to 8451 kJ/kmol, which was 1.032% of the chemical exergy.

Cooling water was assumed available at 8 °C, which is a typical year-round temperature at 50–100 m sea depth in southern Norway. The cooling-water temperature rise was assumed to be 10 °C. With a condenser temperature of 24.2 °C (saturation pressure 0.030 bar), this means a temperature difference (LMTD) of 10.5 °C.

As noted above, the air was also assumed to have a temperature of 8 °C, and with pressure 1.013 bar and relative humidity of 82%. This can be a representative condition for a coastal location in southern Norway. In any case at this temperature, the specific humidity is low and it is reasonable to assume that a choice of a lower relative humidity would have insignificant effects on the results.

4.2 Base Case with reforming

The Base Case was defined by choosing the following quantities:

The steam-to-carbon ratio (not including fuel CO_2) was set to 1.64 at the PRE inlet. From an efficiency point of view, a lower ratio is desired, as the surplus steam otherwise could be used in the steam turbine. On the other hand, if the steam-to-carbon ratio is too low, carbonization may occur in the ATR. Therefore, this ratio was chosen to ensure that carbonization was avoided. In addition to the steam that was added, more water vapor will be produced by oxidation in the ATR.

The PRE feed was preheated to 500 °C. Both feed streams to the ATR, *i.e.* air and PRE products, were preheated by the exhaust-gas stream. The temperatures of these two streams (8 and 4) were set to 15 °C below the gas-turbine outlet-stream (24) temperature. The outlet temperature from the ATR was set to 900 °C. The outlet temperature of the WR was set to 25 °C. The pressure of the reformer was determined according to the outlet pressure of the AC, as this delivers air to the ATR.

The turbine-inlet temperature (TIT, ISO definition) was set to 1250 °C in the Base Case, and the AC-outlet pressure was set to 15.6 bar. These values reflect data from the GE 9 FA gas turbine.

The pressure levels in the triple-pressure reheat steam-turbine cycle were 111 bar, 27 bar, and 4 bar, respectively. This is current design practice for large conventional CC plants. A limit for temperatures at the HP and MP steam turbine inlets (streams 26 and 28) was set to 560 °C. Within this limit, the temperature of the steam was set to 15 °C below the exhaust-gas stream temperature.

The cooling of the high-temperature shift-reforming process, *i.e.* heat exchangers H1, H2, and H4, was used for heating and boiling HP water for the steam cycle. That is, with a maximum temperature of 325 °C. This ensures a low temperature in the heat-exchanger, as has been discussed above.

The main issue of this study was to investigate the described concept and details of the thermal plant, *i.e.* the reforming section and the power-generation sections and the integration between these. Thus, the CO_2 separator (ABS) was not investigated in detail. In the simulations, it was assumed that 90% of the CO_2 content was removed (stream 44) in the chemical absorber unit (ABS). The duty in the heat exchanger H5 was assumed to represent the necessary heat of the stripper boiler in the absorption/desorption section. Therefore, the temperature out of heat exchanger H4 (stream 17) was required to be above 130 °C. This, and the throttling of the CO_2 to 1 atm (stream 44), was assumed to emulate a CO_2 separation process with a realistic exergy balance.

The compression of CO_2 was modeled by three compressors with cooling and water flashing after each compressor. The compressor-outlet pressures were 4 bar, 15 bar, and 60 bar, respectively. After each compressor, the flow was cooled to 20 °C and some condensed water vapor was flashed off. The captured CO_2 was assumed to contain a small amount of dissolved water, 1.5%, which was reduced to only 0.015% through the compression. After the third compression, the flow was cooled to liquid state and pumped to 200 bar.

4.3 Variation of fuel composition and environmental temperature

The contents of CO_2 and hydrocarbons of the fuel may have some effect on the results. The fuel of the Base Case had a content of 5.34% CO_2 and 8.11% of higher hydrocarbons (C_{2+}). To indicate these effects, the plant with reforming was simulated in one case with no CO_2 in the fuel, while the remaining species was unchanged, and in one case with pure methane as fuel. Traded natural gas often has a specification that requires the removal of some CO_2 from the raw gas. Particularly, in a liquefaction process for LNG, all CO_2 has to be removed. In these simulations, the molar ratio of steam to carbon in hydrocarbons was maintained. The CO_2 -free-NG case was equal to the Base Case in this respect. For the methane-fuelled case, which did not need a

pre-reformer for higher hydrocarbons, it was chosen to maintain the ratio in front of the ATR, which was 1.61 moles of steam per mole of methane.

The environmental state also influences the utilization. The Base Case had an environmental temperature of 8 °C in the air and cooling water. Two cases were simulated with 4 °C and 12 °C, respectively. In these simulations, the cooling-water temperature increase (10 °C) and the condenser temperature difference (LMTD at 10.7 °C) were kept equal to those of the Base Case. Thus, the condenser pressure was reduced with lower environmental temperature.

In these four cases, the mass flow rate of air to the AC was kept equal to that of the Base Case.

4.4 Variation of parameters

For all the following variation of parameters, the mass flow rate and power of the AC were unchanged. Also the state of the supplied NG was unchanged.

The Base Case was chosen with an AC-outlet pressure of 15.6 bar, or a pressure ratio of 15.4. The power plant was also simulated with AC-outlet pressures of 20, 25, 30, and 40 bar. At the pressures of 30 and 40 bar, the steam for the reformer was extracted from the HP turbine. The temperature of the steam for reforming (stream 35) was thus lower than in the other cases which extracted steam from the MP turbine.

The Base Case had no supplementary firing (SF). As noted above, it is not antecedently obvious that SF is benign to the efficiency of a power plant with an auto-thermal reforming process. The effects were investigated by a series of simulations with increasing amounts of fuel for SF.

An alternative arrangement of ATR feed heating by the ATR products was investigated. This was to reduce the combustion in the ATR and to reduce temperature differences in the cooling of the ATR products. This arrangement requires advanced materials.

The development of gas turbines is mainly an issue of increasing the TIT, which is accomplished by improved turbine-blade materials and localized blade cooling. Simulations were conducted where the TIT was increased from 1250°C to 1350°C and 1450°C at all the five pressure levels specified above. In the computational model, a cooling-air penalty on the gas-turbine efficiency was included.

Finally, also the influence of the steam-turbine inlet temperature was studied.

4.5 Conventional combined cycle

The conventional combined cycle without reforming for CO₂ capture was simulated for a case corresponding to the Base Case, that is, with TIT 1250 °C, AC-outlet pressure 15.6 bar, and maximum steam-turbine inlet temperature at 560 °C. The steam-cycle pressure levels were the same as in the Base Case. This power plant was also simulated with AC-outlet pressures of 20, 25, 30, and 40 bar, respectively, and with TIT increased to 1350°C and 1450°C. In these cases, the NG was expanded from the supply pressure (50 bar) to a pressure that was 25% higher than the turbine-inlet pressure and reheated with low-temperature heat. None of these cases had supplementary firing. The conventional cycle was also simulated in two cases with environmental temperatures at 4°C and 12°C, respectively (cf. Sec.4.3).

5 Results and Discussion

5.1 The Base Case

The process described above was simulated, and an energy and exergy analysis was made. The main process-stream data are shown in Tables 1 and 3. Results for the corresponding conventional CC case without reforming and without CO₂ capture are also shown in Tables 2 and 3. The exergy values in this table are the exergy flow rates divided by the NG fuel chemical exergy flow rates. The T-s diagram of the three-pressure-level steam cycle is shown in Fig. 2.

The heat transfer in heat exchangers and power balances for the turbines, compressors, and pumps are summarized in Table 4 for the Base Case and for the corresponding conventional case (15.6 bar). Here, the heat transfer rates and the power are given in percent of the NG fuel LHV. The exergy transfer rates from the hot side of the heat exchangers are given in percent of the corresponding heat transfer rate and in percent of the NG fuel chemical exergy flow rate. Table 5 shows the corresponding results for an AC-outlet pressure of 40 bar. The utilization of energy and exergy is shown in Table 6 for the Base Case and in Table 7 for the conventional case. Here, mechanical power is the sum of shaft power of the gas turbine, the steam turbines, and the fuel expander when the power to the AC, FC, and water pumps is subtracted. The gross electric power is taken on the generator. The net electric-power output was obtained by subtracting the auxiliary power consumption and the CO₂ compression power from the gross electric power. The utilized exergy is the sum of net electric-power output and the chemical and thermomechanical exergy of the captured and compressed CO₂. The total lost exergy is the sum of irreversibilities, exergy lost by the released flue gas, generator losses, and auxiliary power consumption.

In the tables, the chemical energy, *i.e.* the lower heating value or negative enthalpy of reaction, of the fuel is listed as input. The high pressure (50 bar) has a small effect on the enthalpy. Actually, due to real-gas effects of pressure, the supplied NG had a negative enthalpy (0.11% of the LHV) relative to the environmental pressure. The temperature (4 °C) also had a minor negative contribution (0.02% of the LHV) to the enthalpy relative to the environmental temperature. These minor contributions were included in the simulations. The chemical exergy of NG is listed in the tables and used as a reference for normalizing the results. However, the thermomechanical exergy of the NG is also regarded as input. This was mainly due to the pressure and it accounts for the possibility of obtaining work from a high-pressure gas. This potential is not included in the fuel-energy input of an energy analysis. The make-up water (stream 34, Table 3) also adds some exergy. For the processes with reforming of NG, this mass flow should be equal to that of the steam mixed with NG (stream 35). Consequently, per unit of mass, the input exergy added to NG chemical exergy was slightly larger for the Base Case than for the conventional case. The total of utilized and lost exergy equals the sum of fuel chemical exergy, fuel thermomechanical exergy, and exergy of the make-up water.

The results show that the power plant with NG reforming had considerably lower efficiency. Higher irreversibilities in the process caused the lower utilization. Furthermore, as 3% of the supplied exergy was stored in the captured and compressed CO₂, the net power production was reduced correspondingly.

More detailed distributions of exergy losses are shown in Table 8. The results for the increased pressure ratios are also included in these tables. Here, the main units are listed. From the reformer section, the ATR and heat exchanger H1 are listed separately, while the "Other reforming" figure comprises MIX, PRE, preheating of the feed to the reformers (*i.e.* streams 2, 4, and 8), HTS, LTS, heat exchangers H2, H3, and H4, the pump for stream 36, the mixer for stream 42, and FC. The irreversibility of the condenser includes the exergy rejected with cooling water, and similarly for the coolers of the CO₂ compression.

As expected, it was seen in all cases that the combustor was the main contributor to irreversibility. In the plant with reforming, the irreversibility of the combustor was lower than in the conventional plant. However, the sum of irreversibilities in the reforming process and the combustor was 6-7 % points higher than that of the combustor in the conventional plant. The ATR and the heat exchangers, in particular H1, were the major contributors to the increased irreversibility. Actually, an ATR includes a combustor where some of the pre-

reformed NG feed is burned to heat the reactants in the reforming reactions. Internal heat transfer from reactions is known as a major source of combustion irreversibility. The heat exchangers were operated at relatively high temperature differences as the coolant was compressed or saturated water for the steam cycle.

The single heat exchanger H1 had an irreversibility that was greater than that of the HRSG. H1 was a boiler in which high-pressure water was heated and vaporized to saturated steam (approx. 325 °C), and heated with the high-temperature products (900 °C) of the ATR. This thermodynamically “unwise” arrangement follows engineering practice and, as explained above, is due to the material problems that otherwise would occur. The irreversibility of this unit was 25-30% of the exergy it transferred to the steam. With improved material technology, this heat may be utilized for various things, including superheating of steam or preheating of the ATR feeds.

The increased complexity of the plant also leads to increased pressure losses that otherwise could have been used for power production in an expander. However, this appeared to be a modest contribution to the total figures. The irreversibility of the Base Case due to pressure losses of the gas flowing through the reforming section, the combustor, and the HRSG was estimated to 0.94% of the NG chemical exergy. This figure does not include the flows in the steam cycle. The main contributors were the combustor (0.38%), the shift reactors and heat exchangers H1 to H5 (0.36%), and the ATR (0.10%). These pressure-loss contributions were included in the irreversibilities reported in the tables. For AC-outlet pressures up to 40 bar (see below), these figures were not substantially changed since they depend on the pressure ratio over each unit and not on the absolute pressure.

The auxiliary power consumption was determined to be 1% of the heat transferred to cooling water in the condenser and the intercoolers of the CO₂ compressors. The latter was approximately one-tenth of the former. The auxiliary power of the plant with reforming was slightly higher than that of the conventional plant.

5.2 Fuel composition and environmental temperature

The results with CO₂-free NG showed small but significant changes from the Base Case. The mixture of hydrocarbons of the fuel was exactly the same. The amount of steam (stream 35) per mole of carbon in hydrocarbons was also maintained. The consumption of hydrocarbons and, accordingly, the input LHV, was slightly lower (0.47%) in the CO₂-free-NG case than in the Base Case, while the compressor and turbine power was unchanged in absolute figures. As the hydrocarbons were not mixed with CO₂, the ratio of chemical exergy to LHV was slightly increased.

The net electric power production was 49.1% of the LHV in the case with no fuel-CO₂. This compares to 48.9% of the Base Case. The main contribution to the overall increase was actually that less CO₂ had to be captured and compressed and its total exergy was reduced by 0.15% of the NG chemical exergy. The fraction of hydrocarbons converted in the reforming process and the percentage of captured CO₂ were virtually unchanged. The changes in irreversibilities were small: It was increased in the combustor by 0.10% of the NG chemical exergy and reduced by 0.06% in the ATR, while other changes were smaller.

An interesting aspect to discuss is the marginal energetic cost of CO₂ removal from natural gas. Compared with the case with no fuel-CO₂, the Base Case produced 0.18 MW less electricity. The LHV of extra fuel consumption was 3.96 MW, which could have been converted into 1.94 MW electric power. This total of 2.12 MW electric power was the cost of capturing and compressing 2.20 kg/s CO₂ that was mixed with the hydrocarbons. If not converted to electricity, this corresponds to 4.33 MW LHV. That is, the energetic cost was 0.27 kWh electricity or 2.0 MJ LHV per kg fuel-CO₂ captured and compressed. This figure can be compared with the marginal fuel cost of CO₂ removal from the fuel at an NG processing plant.

The case with pure methane as fuel gave a net electric production of 49.2% LHV. With the higher H-to-C ratio of the fuel, less CO₂ was produced and captured. The fraction of carbon that was captured was close to those of

the Base Case and the CO₂-free-NG case. The captured and compressed CO₂ represented 2.94% of the methane chemical exergy or 0.1 % point less than in the CO₂-free-NG case. Compared with that case, the pure-methane case had higher irreversibilities in the reforming process (0.20% of the fuel exergy) and lower in the combustor (0.25%). Less heat was transferred to the ATR feeds and, accordingly, more heat and exergy (0.45% of NG chemical exergy) were transferred to the steam cycle.

The effect of reducing the environmental temperature, that is, the air and cooling-water temperature, from 8 °C to 4 °C, was an increase in net electric power production by 0.35% of the LHV. The contributions to this improvement were from the AC, which needed less power input (0.6% of LHV) due to denser air, and the steam turbine, which operated over a larger pressure ratio and produced more power (0.2%). On the negative side, the gas turbine produced less power (0.4% of LHV) due to higher fuel consumption to compensate for the lower temperature in the compressed air.

The underlying details are complex. First it should be noted that the chemical exergy varies very little with temperature. The reduction of the environmental temperature from 8 °C to 4 °C, gave a 0.06% reduced specific chemical exergy of the fuel. Ambient air with lower temperature also gave lower temperature from the compressor. This either requires more heat for the ATR feeds or more combustion within the ATR, or both. Therefore, the temperature of the flue gas entering the HRSG was reduced. However, this reduction was less than that of the ambient and, hence, the specific exergy of the flue gas was slightly increased. Also the heat transfer to the steam cycle in the HRSG and the reformer coolers was reduced at lower environmental temperature, while the corresponding exergy-to-heat ratio and the exergy transfer was increased. The power of the HP and MP steam turbines were somewhat reduced due to lower temperature of the flue gas, whereas the LP-steam-turbine gave some more power due to the lower condenser pressure.

The case simulated with environmental temperature increased to 12 °C gave approximately the same changes, although with the opposite sign. The changes observed were modest, however, they were significant. The nearly 0.1% efficiency decrease per degree of increased environmental temperature cannot be linearly extrapolated to the much higher ambient temperature of sub-tropical and tropical locations. However, the results are a clear indication of how the performance of the plant depends on the climate of the location.

Also for the conventional CC, the reduction of air and cooling-water temperatures from 8 °C to 4 °C gave a 0.35% increase in net electricity production divided by LHV. Here, the AC power input was reduced with 1.6% of LHV, while the gas-turbine power output decreased with 1.2% of LHV. Increasing the environmental temperature from 8 °C to 12 °C gave approximately the same changes with the opposite sign.

5.3 Increased gas-turbine pressure ratio

Details of the process were studied to explain the decreased utilization with the higher pressure ratio reported in Tables 6 to 8. As shown in Fig. 3, the power produced per molar flow rate of H₂ burned in the combustor increased with higher pressure. However, the irreversibility in the reformer per mole of H₂ also increased, as seen in Fig. 4. This effect occurs in the ATR. The figure shows the increased irreversibility of the ATR per mole of H₂ produced in that unit. For the other units of the reformer section, the irreversibility per mole of H₂ produced showed only minor changes. As will be discussed below, the increased pressure ratio required more natural gas to be burned with air to produce the same amount of H₂. Thus, the content of nitrogen and combustion products, CO₂ and H₂O, in the reformed mixture increased with pressure, Table 9. More oxygen was consumed in the ATR, while the accompanying nitrogen dilutes the reformer product. The increased combustion in the ATR was mainly to compensate for the reduced heat transfer from the flue gas, which exited the turbine at a lower temperature. The temperatures of the flue gas at the turbine outlet and at the HRSG inlet (that is, the preheater outlet) are also shown in Table 9. Both the increased pressure and the increased amounts of combustion products (CO₂ and H₂O) tend to reduce the conversion to H₂.

The reduced heat transfer provided to the reformer feeds led to a higher consumption (*i.e.* combustion) of NG in the reformer (ATR) and, consequently, to a higher irreversibility in the system. In the conventional GT cycle, the efficiency could increase with some steps of increased pressure. On the other hand, the pressure increase had a less pronounced effect on the steam cycle of the reforming case than in the conventional case. This was because in the conventional case, the turbine outlet flow enters the HRSG directly. The temperature of the flue gas after preheating the reformer feeds was less reduced by the pressure increase than the GT-outlet temperature (cf. Table 9). This contributes to the reduced efficiency of the conventional plant at the higher pressure levels.

Another observation is about the species molar fractions of the ATR: The steam-to-carbon ratio of the reformer-section inlet (stream 2) was kept constant over the series of simulations. As seen in Table 9, the H₂O-to-C ratio after the ATR (stream 11) increases with higher pressure, that is, following increasing combustion in the ATR. This indicates that at higher pressure levels, the inlet steam-to-carbon ratio can be reduced. Some of the required H₂O may be provided by combustion in the first part of the ATR. Reducing the steam addition (stream 35) could reduce irreversibilities and increase power production. However, this modification has to be based on detailed knowledge of the flow field and the spatial distribution of reactions in the ATR, for instance from computational fluid dynamics (CFD).

One of the "2nd law commandments" (No. 4) of Leites et al. [16] states that if the volume increases, it is necessary to raise (not to reduce) the pressure in order to minimize the irreversibility. In the present process, the volumetric rate increased through the ATR. When the pressure was raised, the irreversibility increased. This may seem to be contradictory to their commandment. However, when looked at closer, this is not the case. As shown in Table 9 and discussed above, the temperature of the ATR feeds was reduced and more heating was required as the pressure was increased. This additional heating, that is, additional combustion in the ATR, to bring the feed to the feed temperature of the Base Case (598 °C) was estimated separately. It was found that the associated exergy loss was larger than the overall increase of irreversibility in the ATR seen in Table 8. Therefore, if given the same feed temperature, increased pressure would reduce, not increase, the irreversibility of the ATR. Thus, the results here are in accordance with the fourth commandment of Leites et al. However, in our process the increased pressure reduces the amount of thermal energy available for the required heating of the ATR feeds, and the overall irreversibility increases.

5.4 Effects of supplementary firing

Above, it was seen that the ATR required substantial amounts of combustion to heat the feeds to the reactor temperature and to heat the endothermic reaction. An alternative or supplement to combustion within the ATR is supplementary firing (SF) in the flue gas in front of the preheating section prior to the HRSG. For a conventional CC plant, it is known that SF reduces the efficiency. However, this is not so obvious for the process given in Fig. 1. The alternative to SF, more combustion in the ATR, implicates increased extraction of air from the gas-turbine compressor to the ATR. This also decreases the efficiency of the CC.

The influence of supplementary firing was investigated by a series of simulations with an increasing amount of fuel burned in the flue gas after the gas turbine. This flue gas was used for preheating feed to the reformers before heating steam and water in the HRSG. Results from different cases of supplementary firing are shown in Fig. 5 and Table 10. The amounts of fuel for SF are given in percentage of the amount of fuel to the GT. The irreversibilities are collected into five groups: the GT system comprising the NG expander, the FC, the AC, the combustor, and the turbine; the ST system comprising the HRSG, the steam turbines, and the condenser; the reforming process; and the WR and CO₂ capture and compression. The burner for supplementary firing is given as a separate unit in the table. It is seen that the relative irreversibilities of both the GT system and the reforming process were reduced with supplementary firing. The GT-system irreversibility per mole of fuel used in the GT combustor showed only minor changes. The reformer irreversibility per mole of fuel reformed was reduced.

The temperatures in the GT exhaust gas after SF are shown in Fig. 6 as a function of the AC-outlet pressure for the different amounts of fuel to SF. This is before heat exchange with the reformer feeds. For each pressure, the values for zero SF also show the temperature before SF, that is, the turbine-outlet temperature. The temperature increase due to SF was virtually linear with the amount of fuel for SF. However, the increase was reduced with increasing pressure: With 10.4% SF, the temperature increase was 82.6 K for the AC-outlet pressure of 15.6 bar and 71.7 K for that of 40 bar. This decrease was due to the lower content of combustibles (mainly H₂) in the reformed fuel at higher levels of AC-outlet and reformer pressure.

The main finding from these simulations was that the irreversibility of the SF burner increases more than the reduction in the remaining process. Irreversibility due to throttling in the burner increased with the GT pressure ratio (*i.e.* the pressure after the CO₂ capture). However, this was only 12-15% of the total irreversibility of the SF burner. The main contribution was due to combustion.

The net electric-power production results, Fig. 5, showed a clear tendency towards reduced efficiency with increased SF for all five AC pressures. However, the case of pressure equal to 20 bar with no SF seemed to be an anomaly. A closer inspection showed that the HRSG, or actually the first heat exchanger, the three-fluid HP/MP superheater, had an irreversibility 0.1 % point higher than what should be expected from the other cases. In fact, this is sufficient to explain the anomaly of this case. However, the detailed analysis of temperatures, pressures, and mass flows of this heat exchanger showed no unexpected values compared to the other cases. Thus, it seems that this case by incidence showed an unfortunate combination of operational parameters.

5.5 Product-feed heat exchange in the autothermal reformer

The analysis of the Base Case above revealed considerable irreversibility in the heat exchanger H1 following the ATR. The high-temperature ATR outflow was cooled by heat exchange with saturated water at a much lower temperature in the HP steam cycle. Such arrangements are common in engineering practice. A thermodynamically more attractive gas-to-gas heat exchanger may lead to material problems at such high temperatures.

If it is assumed that the material problems can be resolved, cooling of the ATR product stream can be used for high-temperature heating. One obvious possibility is to superheat steam instead of boiling in heat exchanger H1. This would reduce the temperature difference, and hence, the irreversibility. However, heating the ATR inflow appears to be more advantageous: The mass flows are equal, the heating capacities are similar, and the temperatures are not far from each other.

In the Base Case, the ATR feeds (streams 5 and 10) had a temperature of 598 °C after preheating by the GT exhaust. The ATR outflow (stream 11) was specified with a temperature of 900 °C. In the following simulations, heat was transferred to the feeds from the products before the latter entered the boiler H1. The amount of heat transfer, and hence, the ATR inlet temperature, was increased in steps as shown in Table 11.

In these simulations, the amount of compressed air was unchanged. Thus, the power and irreversibility rate of the AC were constant. Furthermore, the power production and the irreversibility rates of the turbine and the combustor increased slightly (approximately by 0.5%) in absolute values. The main change was the reduced fuel consumption (6%). This was mainly due to reduced combustion in the ATR.

The irreversibilities are shown in Table 12 in percentage of the NG chemical exergy. The irreversibilities of the AC, the combustor, and the turbine, which were nearly constant in absolute figures, increased relative to the NG chemical exergy according to the reduced fuel consumption (approximately 6%). For these three units together, this was seen as an 1.7%-point increase relative to the NG chemical exergy. As expected, the irreversibilities of the ATR and the heat exchanger H1 were reduced. This reduction was nearly by one-third over the series of variation or 2.8% of the NG chemical exergy. The remaining units had minor changes in

irreversibilities relative to the fuel exergy. For the total system, over this series of cases, the utilized exergy increased by 1.5 % points to 51.0% of the total fuel exergy and the net electric-power production increased by 1.6 % points to 50.5% of the LHV.

As combustion in the ATR was reduced, the outlet gas was less diluted with combustion products and nitrogen from the combustion air. This led to higher concentrations of the reformer products and a shift of the equilibrium composition such that more methane and CO were released from the reforming process (stream 16).

5.6 Increased turbine inlet temperature

In the development of gas turbines, increasing the TIT is an important issue. This is accomplished by improved turbine-blade materials and localized blade cooling. The effect was investigated by simulations where the TIT was increased from the 1250 °C of the Base Case to 1350 °C and 1450 °C. This can be regarded as an extrapolation of the development in gas turbine technology. For each value of the TIT, simulations were conducted with AC-outlet pressure of 15.6, 20, 25, 30, and 40 bar. This was the same pressure variation investigated and described for the Base Case above.

The efficiency in terms of net electric power to the grid divided by the LHV of the consumed NG is shown in Fig. 7. The main result is that the efficiency – as expected – increased with TIT. Furthermore, it is seen that at higher TIT, the efficiency of the plant with reforming was less affected by the pressure ratio than the conventional plant. For the latter, the general tendency was that the efficiency increased with increased pressure ratio.

The corresponding irreversibilities are shown in Figs. 8–9. Here, the units of the plant are collected into four groups (two in the conventional CC cases). When details were inspected, it was observed that the changes in efficiency with higher pressure were a result of reduced irreversibility in the combustor and in the steam-cycle (due to lower temperature of the exhaust inflow to the HRSG), counteracted by increased irreversibility in the AC and the turbine. In the high-pressure cases of the conventional CC, the increased irreversibility outnumbered the reduction. Therefore, the upper three curves in Fig. 7 tend to flatten or turn slightly down. This behavior is known from the literature. It is seen that the irreversibility of the steam cycle is only slightly reduced at the high pressure ratios and not sufficient to compensate for the increased irreversibility in the gas turbine. It may be that the low exhaust-gas temperature at this high pressure ratio requires changes in the heat- and mass-flow configuration of the HRSG for optimum performance. Further studies are required to clarify these relations.

These observations were also made for the plant with reforming and CO₂ capture. Here, the changes in the irreversibility of the turbine and the compressor versus that of the combustor more or less counteracted each other. However, the prominent effect in these variations was the irreversibility of the reforming process. In particular, the irreversibility of the ATR increased by approximately 1.0% of the fuel chemical exergy for all three TITs (from 8.5%, 8.0%, and 9.0%, respectively) as the compressor pressure was increased from 15.6 bar to 40 bar. The reason for this increase was the increased combustion of fuel in the ATR, as discussed above.

Details of the energy and exergy utilization for the Base Case (AC-outlet pressure 15.6 bar, no SF) with increased TIT are shown in Table 13, while Table 14 shows the corresponding breakdown of irreversibilities. As expected, the increased TIT reduced the irreversibility both in the combustor and the rest of the gas-turbine cycle. Due to the higher turbine-outlet temperature, the reforming process also showed a reduction in irreversibility. Here, a 1.1 % point reduction was noted in the ATR together with the heat exchanger H1 and a 0.2 % points increase in the preheater. The remaining units of the reformer section showed only minor changes. Also the HRSG showed slightly reduced irreversibilities, mainly due to the higher temperature of the flue gas.

The effects of increased TIT on irreversibilities in the conventional combined cycle were somewhat different, as seen in Table 15. Here, the reductions in the combustor and the gas-turbine were larger than in the plant with

reforming. On the other hand, the HRSG showed a marked increase, contrary to the power plant with reforming. A major reason for the latter was that the limit imposed on the steam-turbine inlet temperature (560 °C) prevented the increased flue gas temperature to be fully utilized.

Tables 13 and 14 present the case that combines the advantages of increased TIT and heating of the ATR outlet-inlet heat exchange (cf. the previous section). Here, the TIT was 1450 °C, the AC-outlet pressure 15.6 bar, and the ATR feed was heated to 880 °C by heat exchange with the ATR products (900 °C). The effects seen were similar to those discussed in the previous section.

A general observation for both the plant with reforming and the conventional plant is that also with the increased TIT, the combustor and other reactors continue to be the dominating cause of irreversibility in a power plant.

5.7 Increased steam-turbine inlet temperature

As with the gas turbine, the maximum temperature may be a limiting condition in the steam turbine. In order to investigate the influence of this limit, simulations were made where the steam-turbine inlet temperature was increased from 560 °C to 600 °C and 630 °C. Here, the advances of ATR outflow-inflow heat exchange and increased TIT were anticipated. That is, the ATR feed was heated to 880 °C by the ATR products and the TIT was 1450 °C. The AC-outlet pressure was 15.6 bar.

The effect of this was small but significant: a rise in efficiency of 0.3% of the NG LHV. The flow rates of air and NG were not changed. The operation of the reactors and the gas turbine was slightly affected or not affected at all. The main change was that the mass flow of the steam cycle was reduced, as it operated at a greater temperature interval with approximately the same amount of available heat. The corresponding reduction in irreversibility occurred mainly in the heat transfer from flue gas to steam.

5.8 Real-gas effects

In all simulations presented here, the flowing gas was modeled with a real-gas equation of state. Often, the gas flowing through reformers and combustors is modeled as an ideal gas. The value of the compressibility factor, $Z=pv/RT$, will give an indication of the applicability of the ideal-gas approximation. In the Base Case simulations for AC-outlet pressure 15.6 bar, the deviation from unity of the compressibility factor was less than 0.01, except for streams 1, 2, and 3, which had Z values equal to 0.951, 0.982, and 0.978, respectively. For an AC-outlet pressure of 40 bar, the compressibility factors in streams 1, 2, and 3 were 0.876, 0.847, and 0.921, respectively. The factor was 1.021 for streams 22 and 23, and within 0.015 deviation from unity for the remaining gas streams. For all cases, the NG feed (50 bar) had a compressibility factor of 0.855. These findings indicate that an accurate simulation of the reforming process requires a real-gas model.

5.9 Carbon conversion and separation

The purpose of this study was to investigate the thermal process and the integration between the reforming process and the power cycles. For the CO₂ separation process, a relatively simple model was used. The exergy that was available for the separation is seen as the sum of the chemical exergy of the captured CO₂ and the irreversibility of the absorption process. The irreversibilities obtained with this model were comparable to those reported in [8,9]. A modest optimization is possible, in particular since the exergy of low-temperature heat can replace the exergy of the throttling process in the model and avoid some of the power input in the subsequent CO₂ compression.

A more interesting result in this respect is the content of CO₂ versus other forms of carbon and the concentration of CO₂ in the reformed fuel prior to separation (stream 17). These figures are important for the possibilities of achieving certain goals of carbon capture and for the exergetic cost of separation.

In the simulations, a higher percentage of captured CO₂ could have been assumed. However, the carbon present in the form of CO or hydrocarbons will in any case end up as CO₂ in the atmosphere after the combustion. The different variations discussed above showed opposite and competing effects on the conversion of hydrocarbons and CO to CO₂. Reduced combustion in the ATR lowered the amount of combustion products, CO₂ and H₂O, which entered the equilibrium balances. Dilution with nitrogen was reduced, which in turn reduced the conversion of methane to CO and H₂. Increased pressure also affected this conversion.

Higher concentrations of a species reduce the exergetic cost of its separation. However, in the simulations, the molar fraction of CO₂ in the reformed fuel after the WR (stream 19) showed small changes. The Base Case gave 17.4% CO₂ in this stream. This figure was slightly reduced (by 0.3% points) at increased pressure. However, a rise in TIT or SF gave insignificant increases, while the ATR product-to-feed heat exchange resulted in a small increase (by 0.3 % points) over the series of variations discussed above.

The total effect of pressure increase was a reduced ratio of CO₂ to all carbon (CO₂, CO, and methane) after the reforming process. Figure 10 shows this CO₂-to-C ratio as a function of AC outlet pressure for the three different TITs. For the cases with TIT 1250 °C and no SF, the reduction was from 96.0% at AC-outlet pressure 15.6 bar to 94.2% at 40 bar, as shown in Table 9. For the cases with TIT 1450 °C, the reduction was from 94.7% to 92.6% for the corresponding pressure increase.

Supplementary firing also reduced the conversion to CO₂. For TIT 1250 °C and pressure 15.6 bar, the CO₂ was reduced from 96.0% to 95.3% of all carbon over the increase of SF reported above. At pressure 40 bar, the reduction was from 94.2% to 93.1%.

The ATR product-to-feed heat exchange for TIT 1250 °C and pressure 15.6 bar reduced the CO₂-to-C ratio from 6.0% to 94.0% when the feed preheat was increased from 598 °C to 800 °C. Finally, in the case with TIT 1450 °C and ATR feed preheated to 880 °C, the ratio of CO₂ to all carbon after reforming was reduced to 92.9%. In the latter case, nearly 97% of the CO₂ would have to be separated in the ABS achieve 90% carbon capture.

The conversion of hydrogen in hydrocarbon and water vapor to H₂ is shown in Fig. 11. The fraction of all hydrogen found in H₂ decreased with increased pressure and increased with TIT. Furthermore, it was reduced with SF and increased with the ATR product-to-feed heat exchange. These changes followed the changes in ATR combustion discussed above.

5.10 Improvements

Increasing the effective TIT, and thus reducing the combustor irreversibility, seems to be the most prominent measure for improving the efficiency for combined cycles with and without reforming. This is an ongoing development in the gas-turbine industry. Nevertheless, it is worth noting that although there were some improvements, the combustor remained the main source of irreversibility in both the power plant with CO₂ capture and the conventional power plant.

The second measure in the plant with reforming appears to be to improve the heating of the ATR feed by using heat from its products. The drawback of both these improvements is that the amount of carbon converted to CO₂ is reduced. To a limited extent the conversion of CO to CO₂ can be improved by reducing the temperature of the LTS. Furthermore, a reduced temperature in the ATR will shift the equilibrium composition from methane to CO and H₂. However, this will require a catalyst that works at a lower temperature ATR. Since a

lower temperature reduces the possibility of conversion to solid carbon (carbonization) this may allow lower amounts of steam for the reformer.

A third measure is to reduce the amount of steam used in the reforming process (stream 35). This would reduce the need for ATR-feed preheating and combustion in the ATR. On the other hand, this will increase the risk of carbonization in the reformer. As less water vapor from combustion also decreases the possibility of reducing the amount of steam, this possibility for improvement has to be utilized with care and based on detailed studies of the reactor.

As a general possibility, Leites et al. [16] recommend the recirculation of some products as a means to improve 2nd-law efficiency. In the present case, some of the fuel mixture after ABS and FC (stream 20-23) could have been recirculated into the ATR to increase the conversion of methane to CO and CO₂, and hence, improve the separation of CO₂. This feed could have been heated by the correspondingly increasing ATR-product mass flow. Here, the recirculation would increase the heat-transfer irreversibilities and require some compressing. The total effect of this and other possible re-configurations would have to be investigated by further simulations.

The steam cycle may show possible improvements by adjusting the configuration and relations between the different mass flows. However, this section of the plant contributed only a minor part of the irreversibilities, and the potential improvements are limited.

6 Conclusions

A power-plant concept with decarbonization of natural gas (NG) by auto-thermal reforming and precombustion CO₂ removal has been investigated. An energy and exergy analysis has been performed, and the influences of some parameters have been studied. This concept has also been compared to a conventional combined-cycle process.

For the combined-cycle with fuel reforming and CO₂ capture, a turbine-inlet temperature (TIT) of 1250 °C and air-compressor (AC) outlet pressure of 15.6 bar, the net electric power was 48.9% of the LHV of the supplied NG. The exergy analysis showed that the net electric-power output and the exergy of the captured and compressed CO₂ represented 46.9% and 3.1%, respectively, of the chemical exergy of the supplied NG. In the corresponding conventional combined cycle with no CO₂ capture, the net electric power was 59.2% of the LHV and 56.5% of the chemical exergy of the fuel.

The exergy method, contrary to 1st-law analysis, localizes and quantifies the thermodynamic losses (irreversibilities). The main contributions to irreversibility were the combustor (20.5% of the NG chemical exergy) and the autothermal reformer (8.5%). This compares to the combustor (28.7%) in the conventional plant without reforming. Thus, some of the combustor losses in the conventional plant were relocated to the reformer in the new plant.

Increasing the gas-turbine pressure ratio may improve the performance of conventional combined-cycle processes. However, this was not the case for the process with NG reforming and CO₂ capture. The gas turbine yield per amount of fuel consumed in the gas turbine increased with an elevated pressure ratio. As the lower flue-gas temperature required more internal combustion in the reformer, this led to higher total irreversibilities.

It was shown that heating the reforming process by oxidation within the auto-thermal reformer (ATR) is favorable to preheating the reformer feed by supplementary firing (SF) in the gas-turbine exhaust. An increasing amount of fuel to SF raised the total irreversibility, and hence, reduced the net output from the plant. This was due to the higher irreversibility caused by SF compared the reduction of irreversibility of the auto-thermal reforming reactor.

Heating the feeds of the ATR by its products reduced the need for combustion within the ATR, and the associated irreversibilities. Also irreversibilities due to heat exchange were reduced. However, this arrangement requires advanced materials or coatings to avoid material problems.

An increase of the TIT from 1250 °C to 1350 °C and 1450 °C increased the net electric-power production to 50.6% and 52.2%, respectively, of the NG LHV for the plant with reforming and CO₂ capture. The corresponding results for the conventional CC plant were 60.2% and 61.0%. For the plant with reforming and CO₂ capture, a combination of 1450 °C TIT and ATR product-feed heat exchange, gave a net electric-power production of 53.3% of the NG LHV. This makes a difference of 7.7% LHV compared to the conventional plant, including 3.1% stored as exergy in the captured CO₂.

The fraction of hydrocarbons that was converted to CO₂ in the reformer section was reduced both by increasing TIT and by ATR product-feed heat exchange. With a TIT of 1250 °C and AC-outlet pressure of 15.6 bar, the CO₂ contained 96.0% of all carbon after the reforming section, before separation. At a TIT of 1450 °C, the fraction was reduced to 94.7%, and when this TIT was combined with ATR product-feed heat exchange the fraction was reduced to 92.9%. The remaining carbon was present as CO and methane and was combusted to produce CO₂ in the combustor. Consequently, when measures for efficiency improvements are implemented, special care has to be taken not to reduce the overall CO₂ capture of the power plant.

The cases in this study were simulated with a real-gas equation of state. The results indicated that for flows with a high content of water vapor, such as the mixture of natural gas and steam in the reforming process, there are significant real-gas effects. These effects increased with rising pressure.

The combustor appears to be the greatest source of irreversibility both with and without fuel reforming, and its reduction seems to be the primary action for increased efficiency. For the reforming process, reducing heat-transfer temperature differences, as well as the internal combustion in the auto-thermal reformer, will reduce irreversibilities and improve the total efficiency.

References

- [1] Erga O, Juliussen O, Lidal H. Carbon dioxide recovery by means of aqueous amines. *Energy Conversion Management*. 1995;36(6-9):387-392.
- [2] Feron PHM, Jansen AE. The production of carbon dioxide from flue gas by membrane gas absorption. *Energy Conversion Management*. 1997;38(Suppl.):S93-S98.
- [3] Chisea P, Consonni S. Natural gas fired combined cycles with low CO₂ emissions. *ASME J Engineering for Gas Turbines and Power*. 2000;122:429-436.
- [4] Hendriks CA, Blok K. Carbon dioxide recovery using a dual gas turbine IGCC plant. *Energy Conversion Management* 1992;33(5-8):387-396.
- [5] Mathieu P. Presentation of an innovative zero-emission cycle for mitigating the global climate change. In: *Proceedings of the 4th Int. Conf. on Greenhouse Gas Control Technologies, Interlaken, Switzerland, 1999*. p. 615-20.
- [6] Mori Y, Masutani SM, Nihous GC, Vega LA, Kinoshita CM. Precombustion removal of carbon-dioxide from natural-gas power-plants and the transition to hydrogen energy-systems. *ASME J Energy Resources Technology*. 1992;114(3):221-226.
- [7] Audus A, Kaarstad O, Skinner G. CO₂ capture by pre-combustion decarbonisation of natural gas. In: *Proceedings of the 4th Int. Conf. on Greenhouse Gas Control Technologies, Interlaken, Switzerland, 1999*. p. 557-62.
- [8] Lozza G, Chiesa P. Natural gas decarbonization to reduce CO₂ emission from combined cycles. Part 1: Partial oxidation. *ASME J Engineering for Gas Turbines and Power*. 2002;124:82-88.

- [9] Lozza G, Chiesa P. Natural gas decarbonization to reduce CO₂ emission from combined cycles. Part 2: Methane-steam reforming. *ASME J Engineering for Gas Turbines and Power*, 2002;124:89-95.
- [10] Andersen T, Kvamsdal HM, Bolland O. Gas turbine combined cycle with CO₂ capture using auto-thermal reforming of natural gas. In: *ASME Turbo Expo*, München, May 8-12, 2000, 2000-GT-162
- [11] Bolland O, Ertesvåg IS, Speich D. Exergy analysis of gas-turbine combined cycle with CO₂ capture using auto-thermal reforming of natural gas. In: *Power Generation and Sustainable Development*, Liege, Belgium, 8-9 October 2001.
- [12] Kvamsdal HM, Ertesvåg IS, Bolland O, Tolstad T. Exergy analysis of gas-turbine combined cycle with CO₂ capture using pre-combustion decarbonization of natural gas. In: *ASME Turbo Expo*, Amsterdam, 3-6 June 2002. ASME Paper No. GT-2002-30411, 2002.
- [13] Jordal K, Bredesen R, Kvamsdal HM, Bolland O. Integration of H₂-separating membrane technology in gas turbine processes for CO₂ sequestration. In: *Proceedings of the Sixth Int. Conf. on Greenhouse Gas Control Technologies - GHGT-6*, Kyoto, October 2002.
- [14] Kotas TJ. *The exergy method of thermal plant analysis*. 2nd ed. Malabar, FL: Krieger Publishing Company, 1995.
- [15] Kotas TJ. Exergy concepts for thermal plant. *Int J Heat Fluid Flow*. 1980;2(3):105-114.
- [16] Leites IL, Sama DA, Lior N. The theory and practice of energy saving in the chemical industry: some methods for reducing thermodynamic irreversibility in chemical technology processes. *Energy*. 2003;28:55-97.

Table 1 Data for selected positions in the flow sheet in Fig. 1: Molar flow rate, molar weight, and composition (mole fractions) of the streams. Base Case: TIT=1250 °C, AC-outlet pressure 15.6 bar, no SF.

molar flow No.	molewt. (kg/kmol)	H ₂ (%)	CO (%)	CO ₂ (%)	CH ₄ (%)	C ₂₊ (%)	H ₂ O (%)	O ₂ (%)	N ₂ (%)	Ar (%)	
1	1.02	19.67	-	-	5.34	83.89	8.110	0.01	-	2.65	-
2,3	2.78	18.62	-	-	1.96	30.78	2.979	63.31	-	0.97	-
4,5	2.96	17.47	7.85	0.087	4.85	33.03	0.001	53.27	-	0.91	-
6	22.69	28.90	-	-	0.03	-	-	1.00	20.74	77.30	0.92
8,10	2.76	28.90	-	-	0.03	-	-	1.00	20.74	77.30	0.92
9	23.72	27.37	0.00	0.00	0.90	0.00	0.000	13.28	11.06	73.88	0.88
11,12	7.08	18.58	31.39	10.27	5.53	0.18	0.000	21.80	0.00	30.47	0.36
13,14,15	7.08	18.58	38.23	3.43	12.37	0.18	0.000	14.96	0.00	30.47	0.36
16,17,18	7.08	18.58	41.20	0.46	15.34	0.18	0.000	11.99	0.00	30.47	0.36
19	6.24	18.66	46.75	0.52	17.41	0.21	0.000	0.14	0.00	34.57	0.41
20,22,23	5.26	13.94	55.43	0.62	2.06	0.25	0.000	0.16	0.00	40.99	0.48
24,25	23.72	27.37	0.00	0.00	0.90	0.00	0.000	13.28	11.06	73.88	0.88
26,27	5.48	18.02	-	-	-	-	-	100.	-	-	-
28,29	6.95	18.02	-	-	-	-	-	100.	-	-	-
30,33	6.28	18.02	-	-	-	-	-	100.	-	-	-
34,35	1.76	18.02	-	-	-	-	-	100.	-	-	-
36,37,42	4.52	18.02	-	-	-	-	-	100.	-	-	-
38,40	0.78	18.02	-	-	-	-	-	100.	-	-	-
39,41	3.74	18.02	-	-	-	-	-	100.	-	-	-
43	0.84	18.02	-	-	-	-	-	100.	-	-	-
44	0.99	43.61	-	-	98.49	-	-	1.51	-	-	-
45	0.98	43.97	-	-	99.84	-	-	0.16	-	-	-

Table 2 Data for selected positions in a flow sheet simplified from Fig. 1 for a conventional CC case: TIT=1250 °C, AC-outlet pressure 15.6 bar, no SF: Molar flow rate, molar weight, and composition (mole fractions) of the streams.

molar flow No.	molewt. (kg/kmol)	H ₂ (%)	CO (%)	CO ₂ (%)	CH ₄ (%)	C ₂₊ (%)	H ₂ O (%)	O ₂ (%)	N ₂ (%)	Ar (%)	
1	0.90	19.67	-	-	5.34	83.89	8.11	0.01	-	2.65	-
6,7	22.69	28.90	-	-	0.03	-	-	1.00	20.74	77.30	0.92
24,25	23.65	28.47	0.00	0.00	4.49	0.00	0.00	8.47	12.09	74.07	0.88
26,27	4.79	18.02	-	-	-	-	-	100.	-	-	-
28,29	5.47	18.02	-	-	-	-	-	100.	-	-	-
30,33	5.95	18.02	-	-	-	-	-	100.	-	-	-
34	0.	-	-	-	-	-	-	-	-	-	-

Table 3 Data for selected positions in the flow sheet, Fig. 1: Temperature, pressure, chemical exergy flow rate and total exergy flow rate (in % of the chemical exergy flow rate of the NG fuel supplied), lower heating value (in % of the LHV of the NG fuel supplied). Base Case and conventional case: TIT=1250 °C, AC-outlet pressure 15.6 bar, no SF.

No.	Base Case with NG reforming					Conventional case (no reforming)				
	T (°C)	p (bar)	Chem. ex. (% NG chex)	Total ex. (% NG chex)	LHV (% NG LHV)	T (°C)	p (bar)	Chem. ex. (% NG chex)	Total ex. (% NG chex)	LHV (% NG LHV)
1	4.0	16.7	100.	100.76	100.	4.0	19.5	100.	100.80	100.
2	257.7	16.6	101.77	104.68	100.01					
3	500.	16.10	101.77	106.69	100.01					
4	439.9	15.61	101.82	106.31	100.86					
5	598.4	15.14	101.82	107.92	100.86					
6	8.0	1.01	0.	0.	0.	8.0	1.01	0.	0.	0.
7	377.2	15.6	0.	23.97	0.	377.2	15.6	0.	30.80	0.
8	377.2	15.6	0.	3.32	0.					
9	1250.2	15.44	1.85	90.48	0.	1250.0	15.44	2.30	102.89	0.
10	598.4	15.13	0.	4.71	0.					
11	900.2	14.22	85.57	104.11	90.41					
12	350.5	13.80	85.57	93.60	90.41					
13	429.2	13.38	84.06	93.32	88.02					
14	311.6	12.98	84.06	91.47	88.02					
15	200.7	12.59	84.06	90.03	88.02					
16	236.8	12.22	83.53	89.86	86.99					
17	129.7	11.85	83.53	88.72	86.99					
18	25.0	11.75	83.53	87.68	86.99					
22	86.6	19.50	81.63	85.99	86.99					
23	250.0	19.40	81.63	87.03	86.99					
24	613.4	1.02	1.85	26.41	0.	618.1	1.02	2.30	30.58	0.
25	83.0	1.02	1.85	2.60	0.	88.7	1.02	2.30	3.27	0.
26	501.0	111.10	7.01	17.71	0.	560.0	112.10	6.91	18.58	0.
27	312.7	29.17	7.01	13.67	0.	360.7	29.17	6.91	14.18	0.
28	501.0	26.62	8.90	20.85	0.	560.0	28.29	7.91	19.71	0.
29	274.5	4.24	8.03	12.43	0.	308.2	4.24	8.59	13.79	0.
30	24.2	0.03	8.03	2.02	0.	24.2	0.03	8.59	2.19	0.
33	24.2	0.03	8.03	0.47	0.	24.2	0.03	8.59	0.50	0.
34	15.0	3.45	2.25	0.13	0.					
35	435.9	16.7	2.25	4.76	0.					
36	91.5	122.0	5.78	0.84	0.					
37	163.0	121.5	5.78	1.68	0.					
40	325.3	121.0	0.99	1.89	0.					
41	325.3	121.0	4.78	9.11	0.					
44	13.6	1.01	2.14	2.14	0.					
45	47.1	200.	2.14	1.03	0.					

Table 4 Heat and power transfer in the power plant: Energy content (% of NG LHV) and exergy transferred from the hot side (in % of the transferred heat and in % of the NG chemical exergy). Base Case with reforming and conventional case, both with AC-outlet pressure 15.6 bar, TIT=1250 °C.

	Base Case		Conventional case			
	Heat transfer (%LHV)	Exergy (%heat)	Exergy (%chx)	Heat transfer (%LHV)	Exergy (%heat)	Exergy (%chx)
Fuel heater	0.31	0.	0.	0.31	0.	0.
Preheater	8.71	66.52	5.56			
Reformer heat-exchange	25.41	61.27	14.94			
of this: H1	16.05	68.23	10.51			
HRSG	38.92	48.84	18.25	54.13	52.56	27.31
of this: HP/MP	14.52	60.53	8.44	15.93	65.49	10.01
superh.						
Condenser	29.77	5.42	1.55	32.43	5.42	1.69
Intercooling CO2 compr.	3.05					
	Power (%LHV)	Power (%chx)		Power (%LHV)	Power (%chx)	
Fuel expander	0.21	0.20		0.18	0.17	
Air compressor	-30.09	-28.88		-33.96	-32.60	
Fuel compressor	-1.14	-1.09				
Turbine	63.89	61.33		72.12	69.23	
Steam turbines	19.27	18.50		21.92	21.04	
Pumps	-0.20	-0.20		-0.23	-0.22	
CO2 compressors	-1.93	-1.85				

Table 5 Heat and power transfer in the power plant: Energy content (% of NG LHV) and exergy transferred from the hot side (in % of the transferred heat and in % of the NG chemical exergy). Base Case with reforming and conventional case, both with AC-outlet pressure 40 bar, TIT=1250 °C.

	Base Case		Conventional case			
	Heat transfer (%LHV)	Exergy (%heat)	Exergy (%chx)	Heat transfer (%LHV)	Exergy (%heat)	Exergy (%chx)
Fuel heater	0.06	0.	0.	0.	0.	0.
Preheater	3.48	32.37	1.08			
Reformer heat-exchange	27.81	59.66	15.92			
of this: H1	16.95	68.21	11.10			
HRSG	32.92	45.03	14.23	43.86	47.70	20.08
of this: HP/MP	8.02	56.76	4.37	7.34	59.77	4.21
superh.						
Condenser	30.12	5.42	1.57	28.54	5.42	1.49
Intercooling CO ₂ compr.	2.79					
	Power (%LHV)	Power (%chx)		Power (%LHV)	Power (%chx)	
Fuel expander	0.03	0.03				
Air compressor	-55.68	-53.45		-68.63	-65.88	
Fuel compressor	-1.05	-1.01		112.68	108.17	
Turbine	91.02	87.37				
Steam turbine	16.58	15.91		15.46	14.84	
Pumps	-0.20	-0.19		-0.15	-0.14	
CO ₂ compressors	-1.84	-1.77				

Table 6 Energy and exergy utilization and losses for the Base Case (TIT=1250 °C) and increased AC-outlet pressure.

AC-outlet pressure (bar)	15.6	20.0	25.0	30.0	40.0
Fuel LHVflow rate (MW)	834.01	807.66	782.19	757.26	712.44
Mechanical power (MW)	433.15	417.18	403.17	389.37	361.20
Mechanical power (%LHV) ^a	51.94	51.65	51.54	51.42	50.70
Gross electric power (%LHV)	51.21	50.93	50.82	50.70	49.99
Auxiliary power (%LHV)	0.40	0.40	0.40	0.40	0.40
CO2-compression power (%LHV)	1.93	1.92	1.90	1.88	1.84
Net electric power (%LHV)	48.88	48.61	48.52	48.42	47.75
Fuel chemical exergy flow rate (MW)	868.82	841.38	814.84	788.87	742.18
Other exergy inflow (%chx) ^b	1.15	1.15	1.15	1.15	1.15
Mechanical power (%chx)	49.85	49.58	49.48	49.36	48.67
CO2-compression power (%chx)	1.85	1.84	1.83	1.81	1.77
Auxiliary power (%chx)	0.38	0.38	0.38	0.38	0.39
Net electric power (%chx)	46.92	46.66	46.58	46.48	45.83
Exergy in CO2 (%chx)	3.17	3.17	3.16	3.14	3.11
Chemical exergy in CO2 (%chx)	2.14	2.13	2.13	2.12	2.10
Utilized exergy (%chx)	50.09	49.83	49.74	49.62	48.95
Utilized exergy (%tx) ^c	49.58	49.32	49.23	49.11	48.45
Total irreversibility (%chx)	47.29	47.55	47.65	47.77	48.41
Exergy outflow (%chx)	2.67	2.67	2.68	2.67	2.72
Gener. loss and auxil. power (%chx)	1.08	1.08	1.08	1.07	1.07
Total lost exergy (%chx)	51.04	51.30	51.40	51.52	52.19

a: %LHV = percent of fuel (NG) lower heating value (fuel LHV). b: %chx = percent of fuel (NG) chemical exergy

c: %tx = percent of fuel (NG) total exergy at supply state.

Table 7 Energy and exergy utilization and losses for the conventional case (TIT=1250 °C) with increased AC-outlet pressure.

AC pressure (bar)	15.6	20.0	25.0	30.0	40.0
Fuel LHVflow rate (MW)	738.85	700.48	663.65	631.79	578.04
Mechanical power (MW)	443.59	422.17	399.63	379.25	343.21
Mechanical power (%LHV) ^a	60.04	60.27	60.22	60.03	59.37
Gross electric power (%LHV)	59.20	59.42	59.37	59.19	58.54
Auxiliary power (%LHV)	0.32	0.31	0.30	0.30	0.29
Net electric power (%LHV)	58.87	59.11	59.07	58.89	58.26
Fuel chemical exergy flow rate (MW)	769.69	729.72	691.35	658.16	602.17
Other exergy inflow (%chx) ^b	1.02	1.02	1.02	1.02	1.02
Mechanical power (%chx)	57.63	57.85	57.80	57.62	57.00
Auxiliary power (%chx)	0.31	0.30	0.29	0.28	0.27
Net electric power (%chx)	56.51	56.74	56.70	56.53	55.92
Utilized exergy (%chx)	56.51	56.74	56.70	56.53	55.92
Utilized exergy (%tx) ^c	55.94	56.17	56.13	55.95	55.35
Total irreversibility (%chx)	40.12	39.75	39.69	39.75	40.14
Exergy outflow (%chx)	3.27	3.41	3.53	3.64	3.88
Gener. loss and auxil. power (%chx)	1.12	1.11	1.10	1.09	1.07
Total lost exergy (%chx)	44.51	44.28	44.31	44.49	45.09

a: %LHV = percent of fuel (NG) lower heating value (fuel LHV). b: %chx = percent of fuel (NG) chemical exergy
c: %tx = percent of fuel (NG) total exergy at supply state

Table 8 Distribution of exergy losses (in % of NG chemical exergy) on different sections of the system, Base Case and conventional case for increasing AC-outlet pressure (TIT=1250 °C).

AC-outl. press. (bar)	Base Case					Conventional case				
	15.6	20	25	30	40	15.6	20	25	30	40
Air compressor	1.56	1.75	1.94	2.11	2.42	1.76	2.02	2.28	2.53	2.98
Combustor	20.55	19.87	19.26	18.83	18.20	28.74	28.10	27.55	27.11	26.46
Turbine	2.74	3.18	3.43	3.74	4.31	3.08	3.56	4.04	4.48	5.32
Fuel	0.08	0.05	0.04	0.02	0.01	0.06	0.04	0.03	0.01	-
expander/heater										
HRSG	2.12	2.14	2.05	2.05	2.14	2.83	2.59	2.48	2.41	2.35
ST	1.78	1.73	1.70	1.71	1.69	1.96	1.83	1.74	1.66	1.54
Condenser	1.55	1.54	1.52	1.55	1.57	1.69	1.62	1.58	1.54	1.49
ATR	8.52	8.80	9.08	9.32	9.65					
H1	2.79	2.85	2.90	2.84	2.84					
Other reforming	3.32	3.18	3.10	3.05	2.98					
WR	0.40	0.41	0.41	0.41	0.41					
ABS	1.09	1.28	1.46	1.38	1.45					
CO ₂ compression	0.80	0.79	0.79	0.77	0.75					
Sum irreversibilities	47.29	47.55	47.65	47.77	48.41	40.12	39.75	39.69	39.75	40.14
Flue gas exergy	2.67	2.67	2.68	2.67	2.72	3.27	3.41	3.53	3.64	3.88
Sum	49.96	50.23	50.33	50.44	51.13	43.39	43.17	43.21	43.39	44.01

Table 9 Temperatures (°C) and molar ratios in selected streams for the plant with reforming at increasing AC-outlet pressure. Temperatures for the conventional CC plant.

AC-outlet pressure (bar)	15.6	20	25	30	40
Reforming plant					
Temperature (°C) of GT outlet (stream 24)	613.4	570.5	528.2	497.1	449.5
Temperature (°C) in flue gas into HRSG	521.0	498.5	475.0	440.7	416.3
Temperature (°C) ATR feeds (5,10)	598.4	555.5	513.2	484.1	434.5
O ₂ -to-C ratio in reformer (streams 1 and 8)	0.51	0.53	0.55	0.56	0.58
H ₂ O-to-C ratio after ATR (stream 11) ^a	1.36	1.41	1.45	1.41	1.54
CO ₂ -to-C ratio (%) after ATR (stream 11)	34.60	35.63	36.54	35.44	38.41
CO ₂ -to-C ratio (%) after reformer (stream 16)	95.96	95.89	95.60	95.14	94.21
CO-to-C ratio (%) after reformer (stream 16)	2.88	2.47	2.19	1.95	1.62
CH ₄ -to-C ratio (%) after reformer (streams 11-16)	1.15	1.65	2.21	2.91	4.17
Conventional CC plant					
Temperature (°C) of GT outlet (stream 24)	618.1	572.6	533.0	501.6	454.0

a: The inflow (stream 3) H₂O-to-C ratio was 1.56 when fuel CO₂ was included and 1.64 when this was excluded

Table 10 Irreversibilities (% of NG chemical exergy) in variation of supplementary firing (in % of the fuel used for GT) and AC-outlet pressure.

AC-outlet pressure	15.6 bar			
SF (%GT fuel)	0.00	2.07	5.43	10.33
GT cycle	24.93	24.56	24.02	23.26
SF burner	-	0.55	1.39	2.50
ST cycle	5.45	5.48	5.56	5.65
Reforming process	14.63	14.52	14.31	14.03
WR, ABS, CO ₂ compr.	2.29	2.29	2.23	2.20
Total irreversibility	47.29	47.40	47.50	47.63
AC-outlet pressure	20 bar			
SF (%GT fuel)	0.00	2.04	5.49	10.30
GT cycle	24.85	24.51	23.93	23.21
SF burner	-	0.57	1.47	2.61
ST cycle	5.40	5.35	5.40	5.50
Reforming process	14.82	14.69	14.46	14.18
WR, ABS, CO ₂ compr.	2.48	2.43	2.42	2.35
Total irreversibility	47.55	47.54	47.69	47.86
AC-outlet pressure	25 bar			
SF (%GT fuel)	0.00	2.04	5.49	10.32
GT cycle	24.66	24.33	23.76	23.05
SF burner	-	0.60	1.54	2.74
ST cycle	5.27	5.31	5.36	5.46
Reforming process	15.08	14.89	14.66	14.34
WR, ABS, CO ₂ compr.	2.65	2.59	2.58	2.52
Total irreversibility	47.65	47.72	47.89	48.10
AC-outlet pressure	30 bar			
SF (%GT fuel)	0.00	2.04	5.49	10.26
GT cycle	24.70	24.36	23.82	23.07
SF burner	-	0.62	1.60	2.82
ST cycle	5.31	5.35	5.42	5.52
Reforming process	15.20	15.04	14.72	14.42
WR, ABS, CO ₂ compr.	2.57	2.53	2.44	2.43
Total irreversibility	47.77	47.90	48.00	48.27
AC-outlet pressure	40 bar			
SF (%GT fuel)	0.00	2.04	5.49	10.31
GT cycle	24.93	24.59	24.06	23.31
SF burner	-	0.65	1.69	3.01
ST cycle	5.39	5.43	5.49	5.58
Reforming process	15.48	15.24	14.86	14.55
WR, ABS, CO ₂ compr.	2.61	2.56	2.48	2.45
Total irreversibility	48.41	48.47	48.59	48.90

Table 11 Energy and exergy utilization and losses for the Base Case (AC-outlet pressure 15.6 bar, TIT=1250 °C, no SF) and with product-feed heat exchange in the ATR

ATR inlet temperature (°C)	598 ^d	650	700	750	800
Fuel LHV flow rate (MW)	834.01	821.95	807.53	794.29	783.78
Mechanical power (MW)	433.15	430.21	426.36	422.13	419.21
Mechanical power (%LHV) ^a	51.94	52.34	52.80	53.15	53.49
Gross electric power (%LHV)	51.21	51.61	52.06	52.40	52.74
Auxiliary power (%LHV)	0.40	0.39	0.38	0.37	0.37
CO ₂ -compression power (%LHV)	1.93	1.92	1.91	1.90	1.89
Net electric power (%LHV)	48.88	49.29	49.77	50.13	50.48
Fuel chemical exergy flow rate (MW)	868.82	856.26	841.24	827.45	816.50
Other exergy inflow (%chx) ^b	1.15	1.15	1.15	1.15	1.15
Mechanical power (%chx)	49.85	50.24	50.68	51.02	51.34
CO ₂ -compression power (%chx)	1.85	1.84	1.83	1.82	1.81
Auxiliary power (%chx)	0.38	0.38	0.37	0.36	0.35
Net electric power (%chx)	46.92	47.32	47.77	48.12	48.46
Exergy in CO ₂ (%chx)	3.17	3.16	3.14	3.12	3.10
Chemical exergy in CO ₂ (%chx)	2.14	2.13	2.11	2.10	2.09
Utilized exergy (%chx)	50.09	50.48	50.91	51.24	51.56
Utilized exergy (%tx) ^c	49.58	49.96	50.39	50.72	51.03
Total irreversibility (%chx)	47.29	46.86	46.36	45.99	45.60
Exergy outflow (%chx)	2.67	2.72	2.78	2.83	2.90
Gener. loss and auxil. power (%chx)	1.08	1.08	1.08	1.07	1.07
Total lost exergy (%chx)	51.04	50.65	50.21	49.89	49.57

a: %LHV = percent of fuel (NG) lower heating value (LHV). b: %chx = percent of fuel (NG) chemical exergy.

c: %tx = percent of fuel (NG) total exergy at supply state. d: Base Case, no product-feed heat exchange in the ATR.

Table 12 Distribution of exergy losses (in % of NG chemical exergy) in different sections of the system for the Base Case (AC-outlet pressure 15.6 bar, TIT=1250 °C, no SF) and with product-feed heat exchange in the ATR.

ATR inlet temperature (°C)	598 ^a	650	700	750	800
Air compressor	1.56	1.58	1.61	1.64	1.66
Combustor	20.55	20.85	21.27	21.62	21.96
Turbine	2.74	2.79	2.84	2.89	2.94
Fuel expander/heater	0.08	0.08	0.08	0.08	0.08
HRSG	2.12	2.04	2.08	2.11	2.14
ST	1.78	1.76	1.73	1.70	1.67
Condenser	1.55	1.52	1.49	1.46	1.43
ATR	8.52	8.25	7.88	7.51	7.18
H1	2.79	2.45	1.99	1.63	1.30
Other reforming	3.32	3.30	3.26	3.25	3.22
WR	0.40	0.40	0.38	0.38	0.37
ABS	1.09	1.06	0.98	0.94	0.89
CO2 compression	0.80	0.80	0.79	0.79	0.78
Sum irreversibilities	47.29	46.86	46.36	45.99	45.60
Flue gas exergy	2.67	2.72	2.78	2.83	2.90
Sum	49.96	49.58	49.14	48.82	48.50

a: Base Case, no product-feed heat exchange in the ATR.

Table 13 Energy and exergy utilization and losses for the Base Case (AC-outlet pressure 15.6 bar, no SF) with increased turbine-inlet temperature (TIT).

TIT (°C)	1250	1350	1450	1450 ^d
Fuel LHV flow rate (MW)	834.01	925.90	1017.80	976.36
Mechanical power (MW)	433.15	496.72	562.37	549.42
Mechanical power (%LHV) ^a	51.94	53.65	55.25	56.27
Gross electric power (%LHV)	51.21	52.90	54.48	55.48
Auxiliary power (%LHV)	0.40	0.39	0.38	0.36
CO ₂ -compression power (%LHV)	1.93	1.92	1.90	1.87
Net electric power (%LHV)	48.88	50.59	52.20	53.26
Fuel chemical exergy flow rate (MW)	868.82	964.56	1060.29	1017.11
Other exergy inflow (%chx) ^b	1.15	1.16	1.16	1.16
Mechanical power (%chx)	49.85	51.50	53.04	54.02
CO ₂ -compression power (%chx)	1.85	1.84	1.83	1.79
Auxiliary power (%chx)	0.38	0.37	0.36	0.34
Net electric power (%chx)	46.92	48.56	50.11	51.13
Exergy in CO ₂ (%chx)	3.17	3.15	3.13	3.06
Chemical exergy in CO ₂ (%chx)	2.14	2.12	2.11	2.06
Utilized exergy (%chx)	50.09	51.71	53.23	54.19
Utilized exergy (%tx) ^c	49.58	51.18	52.69	53.64
Total irreversibility (%chx)	47.29	45.67	44.11	43.05
Exergy outflow (%chx)	2.67	2.66	2.69	2.80
Gener. loss and auxil. power (%chx)	1.08	1.09	1.10	1.10
Total lost exergy (%chx)	51.04	49.42	47.90	46.94

a: %LHV = percent of fuel (NG) lower heating value (LHV). b: %chx = percent of fuel (NG) chemical exergy.

c: %tx = percent of fuel (NG) total exergy at supply state.

d: with ATR-feed preheated to 880 °C by heat exchange with the ATR outlet

Table 14 Distribution of exergy losses (in % of NG chemical exergy) in different sections of the system for the Base Case (AC-outlet pressure 15.6 bar, no SF) with increased turbine-inlet temperature (TIT).

TIT (°C)	1250	1350	1450	1450 ^a
Air compressor	1.56	1.40	1.28	1.33
Combustor	20.55	20.08	19.61	20.54
Turbine	2.74	2.48	2.26	2.37
Fuel expander/heater	0.08	0.08	0.08	0.08
HRSG	2.12	2.02	1.83	2.16
ST	1.78	1.77	1.76	1.70
Condenser	1.55	1.51	1.47	1.41
ATR	8.52	8.00	7.51	6.57
H1	2.79	2.73	2.67	1.53
Other reforming	3.32	3.45	3.55	3.49
WR	0.40	0.38	0.38	0.33
ABS	1.09	1.02	0.96	0.78
CO2 compression	0.80	0.79	0.79	0.77
Sum irreversibilities	47.29	45.70	44.14	43.08
Flue gas exergy	2.67	2.66	2.69	2.80
Sum	49.96	48.36	46.83	45.88

a: with ATR-feed preheated to 880 °C by heat exchange with the ATR outlet

Table 15 Net electric-power production, distribution of exergy losses in different sections of the system for the conventional plant (AC-outlet pressure 15.6 bar) with increased turbine-inlet temperature (TIT).

TIT (°C)	1250	1350	1450
Fuel LHV flow rate (MW)	738.85	837.69	940.92
Net electric power (%LHV)	58.87	60.17	61.04
Net electric power (%chx)	56.51	57.76	58.59
Irreversibilities (%chx)			
Air compressor	1.76	1.55	1.38
Combustor	28.74	27.72	26.74
Turbine	3.08	2.72	2.45
Fuel expander/heater	0.06	0.06	0.06
HRSG	2.83	3.28	3.88
ST	1.96	2.03	2.09
Condenser	1.69	1.71	1.73
Sum irreversibilities	40.12	39.06	38.33
Flue gas exergy	3.27	3.10	2.99
Sum exergy loss	43.39	42.16	41.32

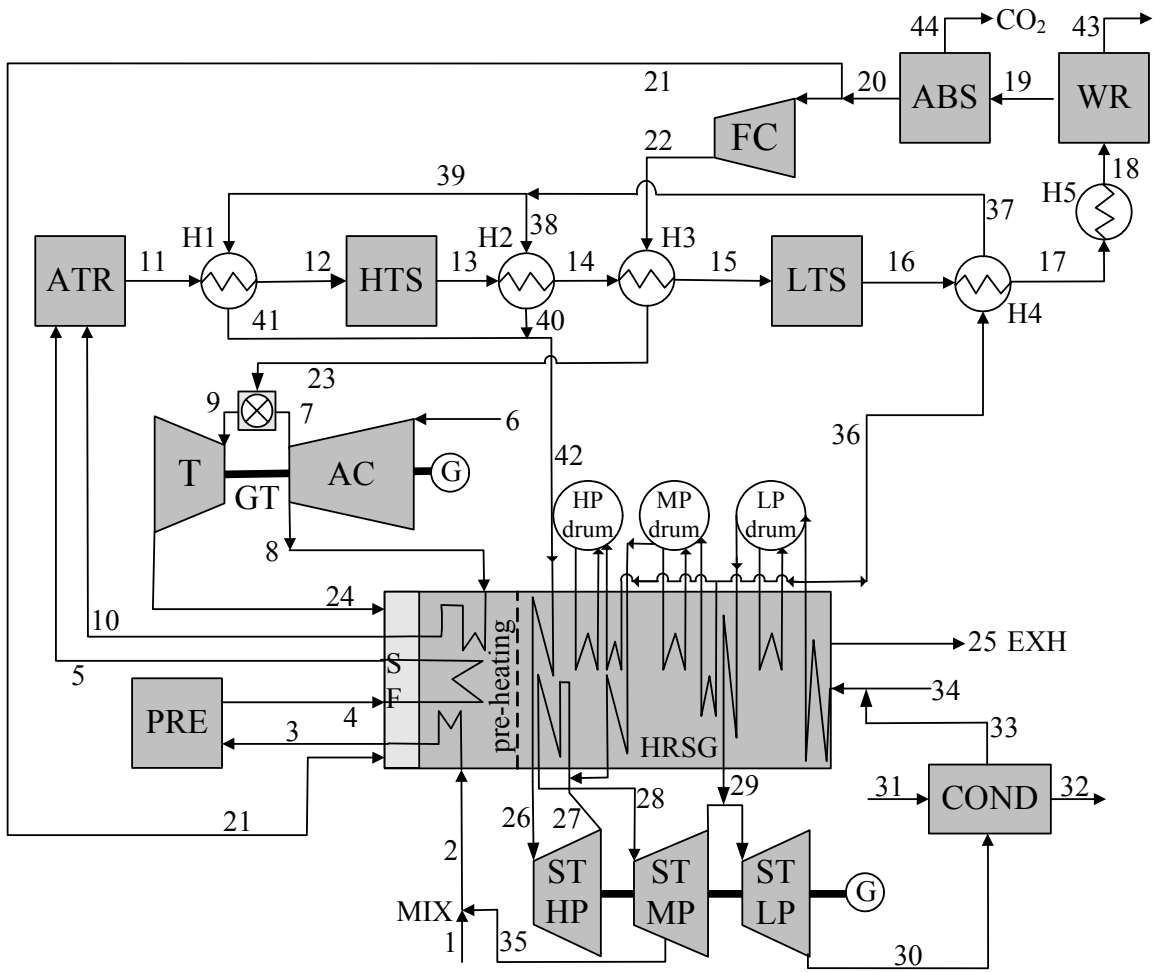


Figure 1 Process flow diagram of the precombustion CO₂-capture power plant.

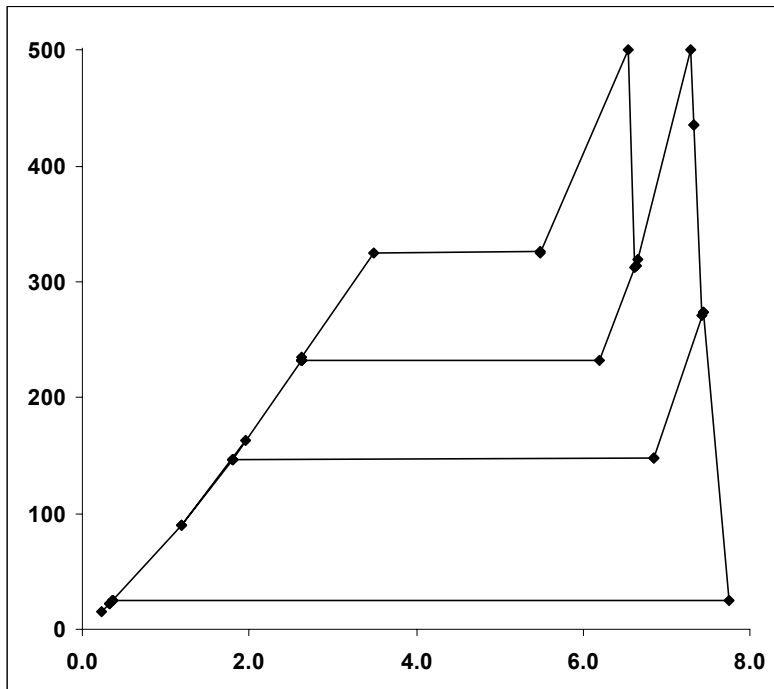


Figure 2 Temperature vs. specific entropy of the steam cycle, Base Case. The entropy is relative to liquid water at the triple point. The number labels show the states corresponding to streams numbered in Fig. 1 and Tables 1-3. High-pressure water heating and boiling are conducted both in the HRSG (states c-e-f, not numbered in Fig. 1) and in the shift-reaction coolers H4, H2, and H1 (36-37-42, with pump before 36). The location of point 35 varies with the AC outlet pressure. In the cases where this is 30 or 40 bar, point 35 is found between points 26 and 27.

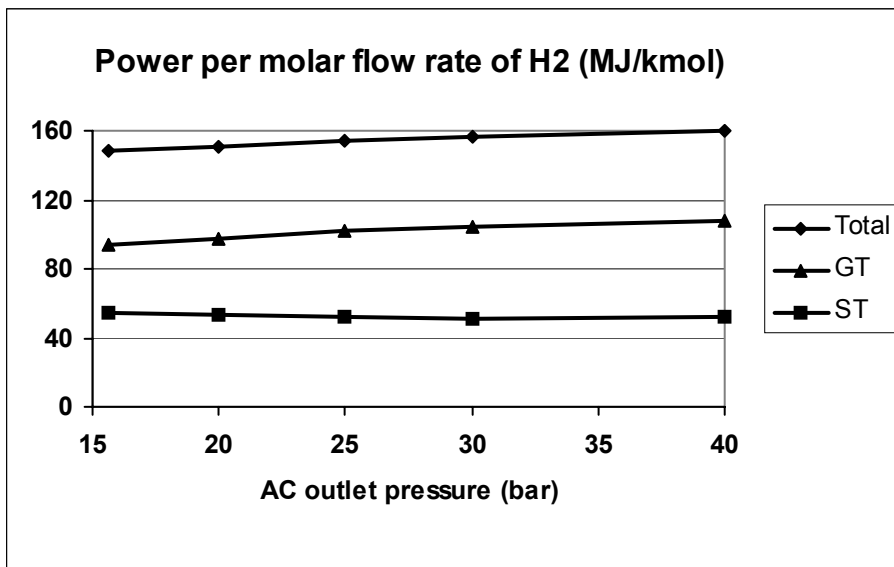


Figure 3 Net mechanical power produced in the total system, by the gas turbine cycle, and by the steam-turbine cycle per flow rate of H₂ in the reformed fuel (MJ/kmol H₂) as a function of AC-outlet pressure (bar).

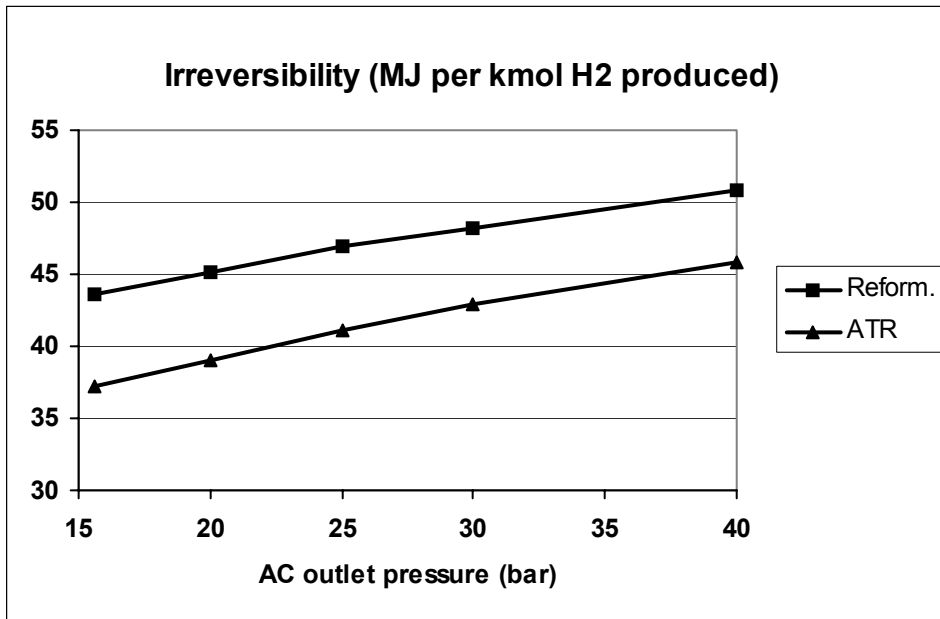


Figure 4 Irreversibility in the ATR and in the entire reformer section, in MJ per kmol H₂ produced as a function of AC-outlet pressure (bar).

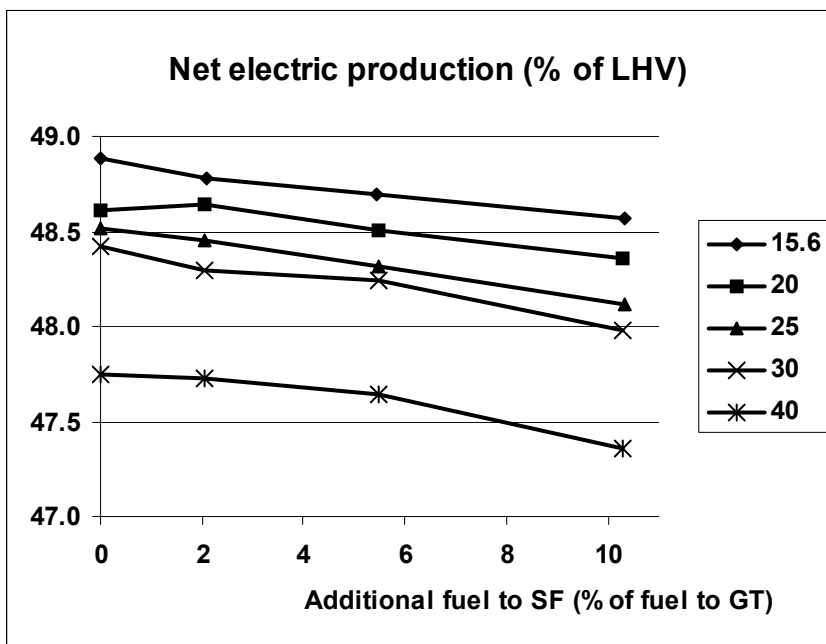


Figure 5 Net electric-power production (in % of the natural gas LHV flow rate) as a function of amount of fuel to supplementary firing (in % of the fuel used in the GT) for five different AC-outlet pressures (bar).

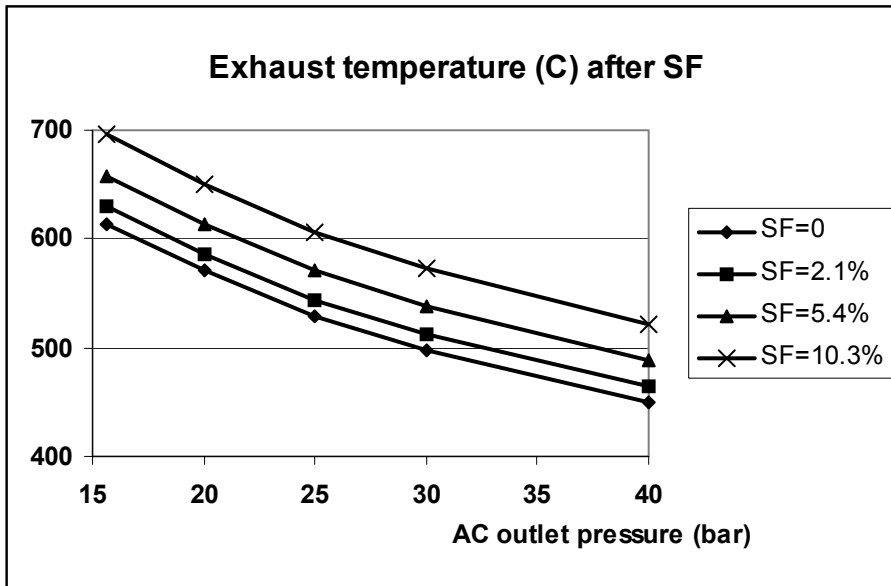


Figure 6 Temperature (°C) in gas-turbine exhaust after supplementary firing, before heat exchange with reformer feed, as a function of AC-outlet pressure (bar) for different amounts of fuel to SF (in % of fuel used for the gas turbine).

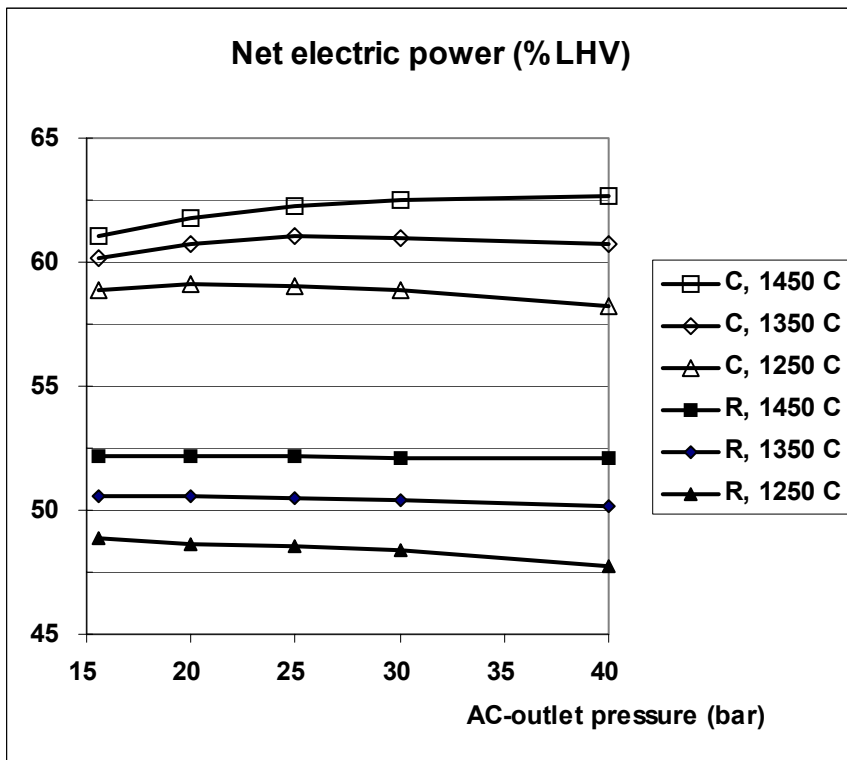


Figure 7 Net electric-power production in percentage of the NG LHV consumption rate as a function of AC-outlet pressure for three different TITs for the conventional plant (C) and the reforming plant (R).

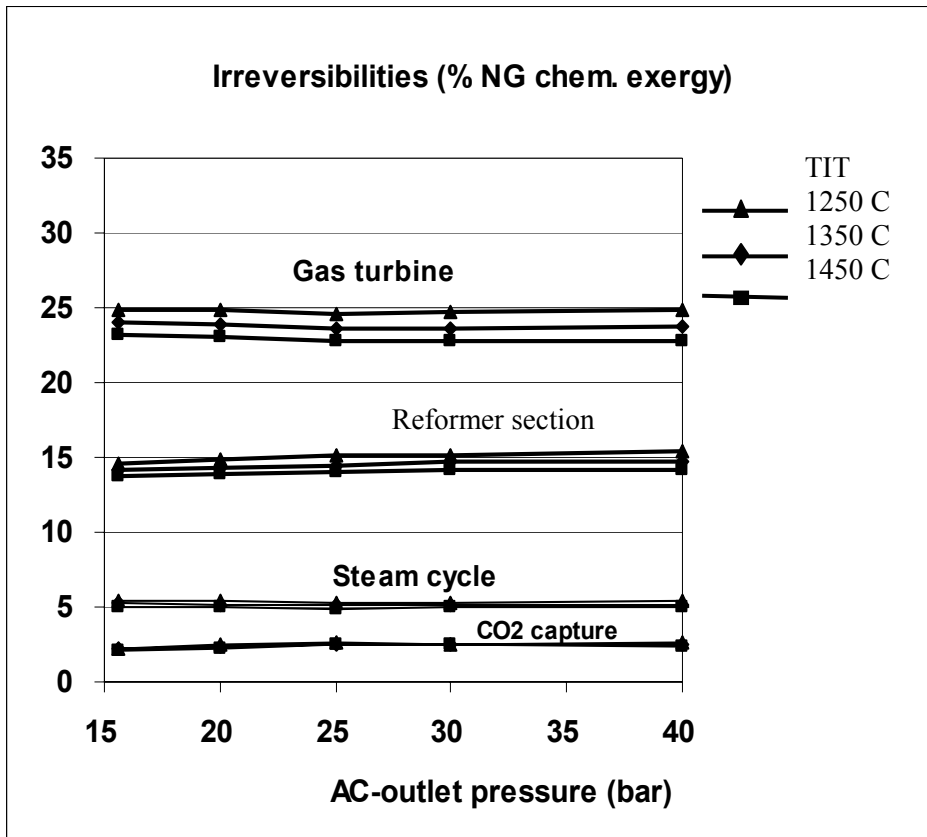


Figure 8 Irreversibilities (in % of NG chemical exergy) for all units in groups for the plant with reforming at three different TITs and various AC-outlet pressures.

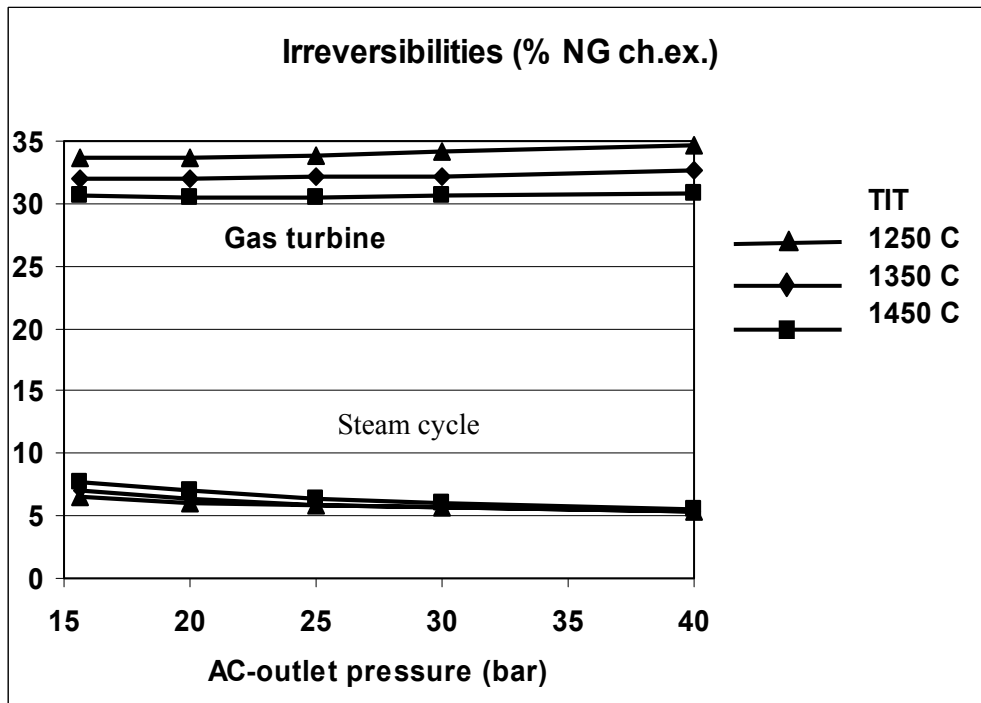


Figure 9 Irreversibilities (in % of NG chemical exergy) for all units in groups for the conventional plant at three different TIT and various AC-outlet pressures.

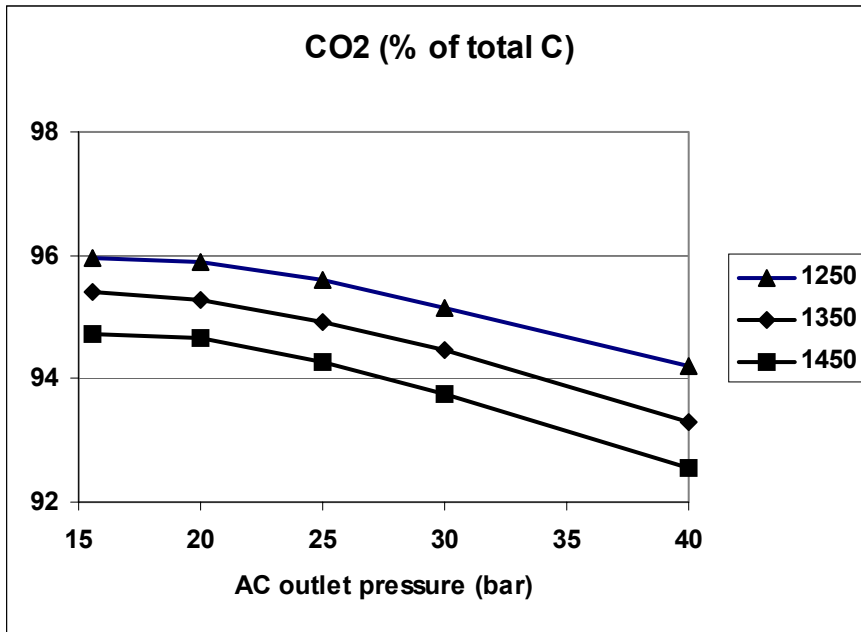


Figure 10 Fraction of all carbon that is present in the form of CO₂ after reforming (stream 17) as a function of AC-outlet pressure for three different TITs.

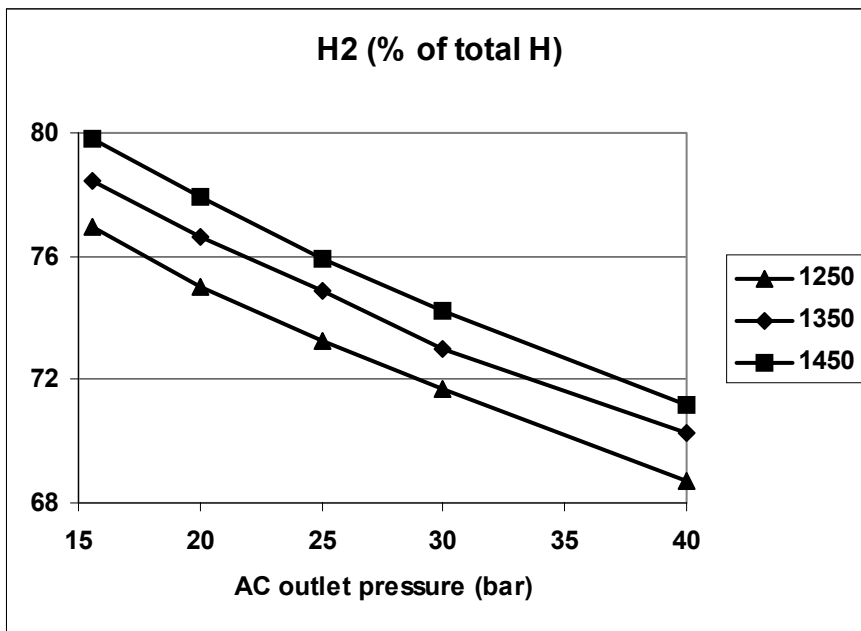


Figure 11 Fraction of all hydrogen that is present in the form of H₂ after reforming (stream 17) as a function of AC-outlet pressure for three different TITs.